PLATES ON ELASTIC FOUNDATIONS SUBJECTED TO MOVING LOADS

Thesis for the Degree of M. S.

MICHIGAN STATE UNIVERSITY

William C. Moody

1965

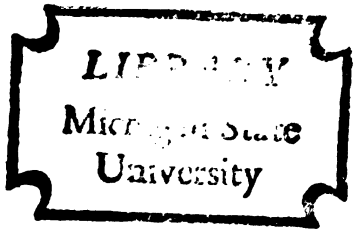

PLATES ON ELASTIC FOUNDATIONS SUBJECTED TO MOVING LOADS

By

William C. Moody

A THESIS

Submitted to
Michigan State University
in partial fulfillment of the requirements
for the degree of

MASTER OF SCIENCE

Department of Civil Engineering

1965

ABSTRACT

PLATES ON ELASTIC FOUNDATIONS SUBJECTED TO MOVING LOADS

by William C. Moody

An analytical study is made of the dynamic behavior of rectangular elastic plates on elastic foundations (of the Winkler type) subjected to moving loads of constant magnitude. The method of analysis is based on a discretization of the plate by a combination of the finite difference and lumped parameters technique. The resulting equations of motion are integrated numerically.

Numerical results are obtained for a 10 ft. x 10 ft. concrete slab, 12 in. thick, and free on all edges. The foundation stiffnesses used are varied to correspond to a practical range of subgrade soil stiffness. Most of the data are for the load moving along one edge of the plate, as this load track produces the largest deflection and bending moment in the plate.

It was found that for speeds less than 70 mph the dynamic effects are rather small. Beyond this speed, the dynamic effects can become appreciable. The maximum deflection generally occurs at the departure corner. The maximum bending moment occurs near the center of the load track. Although an increase in foundation stiffness generally tends to decrease both the values of the maximum deflection and moment, its influence on the maximum moment is substantially smaller than that on deflection.

ACKNOWLEDGMENTS

The author wishes to express his sincere appreciation to his major professor, Dr. Robert K. Wen, for continued guidance and advice not only on this thesis but throughout his graduate studies. Thanks are also due to Dr. Charles E. Cutts, Head, Department of Civil Engineering, for his encouragement.

The author made much use of the facilities of the Computer Laboratory of Michigan State University and wishes to thank the staff and personnel for their assistance.

The author also wishes to take this opportunity to express gratitude to his father whose interest and example provided the ambition which this thesis partially fulfills.

TABLE OF CONTENTS

LIST OF TABLES

LIST OF FIGURES

CHAPTER I

INTRODUCTION

The purpose of this thesis is to study the dynamic behavior of plates on elastic foundations subjected to moving loads. This investigation is limited to rectangular plates subjected to loads of constant magnitude.

Although the above system may represent such structures as pontoon bridges, the chief motivation for the study is to examine the dynamic response of pavements for airport runways and for highways. At the present time such pavements are designed primarily on a static basis. With the advent of heavier loads moving at faster speeds, it seems appropriate that the problem be considered from a dynamic point of view.

The dynamic analysis of plates on elastic foundations is a difficult problem; the case of moving loads is even more so. However, two works based on rather drastic simplifications of the problem have been reported in the literature.

Livesley(5) has investigated the influence of load speed on the response of an infinite plate. Harr (2) also has considered the influence of load speed treating the plate as a single degree freedom system. It is apparent that such simplified systems have only a limited degree of realism in representing the actual physical problem.

The system considered in this thesis is more realistic in that the plate has finite dimensions, practical boundary

conditions, and it can reflect the multi-degree freedom behavior of the structures.

The approach used in this thesis consists of a replacement of a continuous system by a discrete system. This is done by first dividing the plate into a rectangular grid work and then "lumping" the plate properties at the mass or node points. By replacing the space derivatives in the equation of motion by finite difference patterns, the equation of motion for the mass at each mode point is derived. The system of equations is then integrated numerically. Much of this method is described in Reference 9. However, the problem of moving loads was not considered therein. In this thesis, the method of analysis is explained in Chapter II.

In Chapter III the numerical results are presented. The effect on the response of the plate due to the velocity of the moving load, the stiffness of the foundations, and the load tracking is discussed. Also included are the effects of damping.

A summary and some concluding remarks are presented in Chapter IV. The computer program prepared for this study and some notes on its use are presented in the Appendix.

1.3 Notations

The notation listed in the following has been adopted in this thesis. Each symbol is defined when first introduced and is collected here in alphabetical order for convenience of reference. "Fortran" notation is listed separately in the Appendix.

a = length of the longer side of the plate;

A_i = tributary area to point (i);

b = length of the shorter side of the plate;

$\overline{b}$ = vt, distance to front of load from entry edge;

BHO = ∇^4, the biharmonic operator in finite differences form;

c = foundation viscous damping constant;

D = $Eh^3/12\,(1 - \nu^2)$, flexural rigidity of the plate;

d = distance from node point to back of load;

E = modulus of elasticity of plate material;

F_{ij} = $\theta \cdot P_{ij}$, non-dimensional forcing function at point (i,j);

h = plate thickness;

i,j = variable subscripts to denote points in space;

k = foundation stiffness constant;

m = mass per unit area of plate;

M_1 = algebraically larger principal bending moment;

M_2 = algebraically smaller principal bending moment;

M'_1 = $M_1\ a/D$, dimensionless M_1;

M'_2 = $M_2\ a/D$, dimensionless M_2;

M_i = moment at a point (i) derived from derived deflections w_i;

n = a/λ, number of grid divisions;

p_i = load intensity at point (i);

$\overline{P}$ = intensity of moving load in psi;

P_i = concentrated load at point (i);

q = lateral loading of plate;

T_o = $(\frac{ma^4}{D})^{1/2}$; factor to divide t, to make it dimensionless;

T_s = shortest period of the plate system;

t = time;

$\bar{t}$ = time/$(a + \gamma)/v$;

u = $\frac{w}{h}$, dimensionless deflection;

u_{ij} = dimensionless deflection at the point (i,j);

v = velocity of moving load;

$\dot{v}_{ij}$ = $\dot{u}_{ij}$, dimensionless velocity at the point (i,j);

w = deflection;

w_i = deflection at point (i);

$\dot{w}_i$ = dw/dt, velocity at point (i);

$\ddot{w}_i$ = d^2w/dt^2, acceleration at point (i);

x = space coordinate;

y = space coordinate;

α = $\frac{ka^4}{D}$, dimensionless foundation stiffness constant;

β = $\frac{ca^4}{DT_o}$, dimensionless foundation damping constant;

γ = vT_o/a, dimensionless velocity parameter;

Δ = prefix denoting "increment";

∇^4 = biharmonic operator;

λ = grid size;

ν = Poisson's ratio

τ = t/T_o, dimensionless time;

θ = a^4/Dh; factor to be multiplied to P_{ij} to make it dimensionless.

CHAPTER II

METHOD OF ANALYSIS

2.1 General

The governing equation of motion for a plate on an elastic foundation with damping (see Figure 2.1) is given by:

$$\nabla^4 w = \frac{1}{D}[q - kw - c\dot{w} - m\ddot{w}] \qquad (2.1)$$

in which w denotes the deflection of the plate, q denotes the lateral loading, m the mass of the plate, and k and c the stiffness and damping coefficients of the foundation, respectively. The symbol D denotes the flexural rigidity of the plate. The loading q is in general a function of the space variables (x, y) as well as time t, i.e., $q = q(x,y,t)$. If it is moving on the plate, the position of the load is also a function of time, thus $q = q[x(t),y(t),t]$.

An exact solution of the problem of plates on elastic foundations subjected to moving loads is almost impossible except for a few special cases, such as rectangular plates simply supported on all edges. To obtain a solution for plates with free edges, one has to resort to approximate methods. The method used in this investigation consists of a combination of a formal application of finite difference (in expanding the $\nabla^4 w$ term in Equation 2.1), lumped parameters (in treating the other terms in Equation 2.1), and numerical integration (of the equations of motion of the resulting discrete system).

2.2 Discretization of the Equation of Motion

The discretization of the equation of motion is accomplished by first replacing the ∇^4 operator in Equation 2.1 by the finite difference patterns given in Figure 2.8, assuming that the domain of the plate is divided into square grids. There are six general types given, depending on the location of the point on the plate. It should be noted that these patterns shown have already taken into account the free edge boundary conditions of the plate, and involve only the node points on the plate; there is no need to consider any imaginary points outside the domain of the plate.

Denoting these patterns by the symbols BHO (for Biharmonic Operator), for any node point (i), Equation 2.1 may be written as:

$$\frac{1}{\lambda^2}[\text{BHO}]w_i = \frac{1}{D}[P_i + p_i A_i] \qquad (2.2)$$

where λ is the size of grid used, P_i represents the concentrated load at point (i), p_i is the load intensity at point (i), and A_i is the "tributary area" for point (i). For a corner point, $A_i = \lambda^2/4$, and for a typical exterior and interior point, $A_i = \lambda^2/2$ and λ^2, respectively.

For the present problem, P_i will represent the portion of the moving load lumped to point (i). The load intensity p_i includes the foundation forces and the inertia forces:

$$p_i = -(kw_i + c\dot{w}_i + m\ddot{w}_i)$$

Substituting these into Equation 2.1 the discrete form of the equation of motion is obtained:

$$\frac{1}{\lambda^2}[BHO]w_i = \frac{1}{D}[P_i - kw_iA_i - c\dot{w}_iA_i - m\ddot{w}_iA_i] \qquad (2.3)$$

Written out for Point 1 of the plate shown in Figure 2.6, this would be:

$$\frac{1}{\lambda^2}[(-3 + 2\nu + \nu^2)(-w_1 + w_2 + w_{10}) + \frac{1}{2}(1 - \nu^2)(w_2 + w_{10}) +$$

$$(2 - 2\nu)w_{11}] = \frac{1}{D}[P_1 - kw_1\frac{\lambda^2}{4} - c\dot{w}_1\frac{\lambda^2}{4} - m\ddot{w}_1\frac{\lambda^2}{4}] \qquad (2.4)$$

2.3 Treatment of Moving Load

The moving load considered is distributed over an area equal to one square grid panel of the plate. The load moves with a constant velocity v in a direction parallel to one edge. Also, the load intensity $\bar{P}$ remains constant throughout the travel. A schematic diagram of the load-plate system is shown in Figure (2.1).

It is apparent that the load will always be moving in between two rows of node points. To discretize the load, some mechanism for distributing the total load to the various node points must be found. To begin, the load is lumped transversely and considered to be a distributed load of magnitude $\bar{P}\lambda/2$ acting on each of the two rows of grid points as shown in Figure (2.2). Then, this distributed load is replaced by concentrated loads P_i calculated as reactions on the node points assuming that a simple beam spans between two adjacent node points. Thus, at the three points which the load may affect, the concentrated loads are cal-

culated from the following equations (see Figure (2.3)):

$$P_i = \frac{\overline{P}}{4}(\lambda - d)^2$$

$$P_{i+1} = \frac{\overline{P}}{2}(\lambda^2/2 + d\lambda - d^2) \qquad (2.5)$$

$$P_{i+2} = \frac{\overline{P}d^2}{4}$$

When the load begins entering the plate, the concentrated loads may be calculated from a consideration of Figure (2.4) and the equations are:

$$P_1 = \frac{\overline{Pb}}{2}(\lambda - \overline{b}/2) \qquad (2.6)$$

$$P_2 = \frac{\overline{Pb}^2}{4}$$

where $\overline{b} = vt$ denotes the distance between the front edge of the load to the entry edge of the plate. When $\overline{b}$ equals λ, then Equation (2.5) applies.

When the load starts to leave the plate, by Figure (2.5) the equations for P_n, P_{n-1} are:

$$P_n = \frac{\overline{P}}{4}(\lambda^2 - d^2) \qquad (2.7)$$

$$P_{n-1} = \frac{\overline{P}}{4}(\lambda - d)^2$$

2.4 Dimensionless Form of Equations of Motion

In order to facilitate computation, it is convenient to make the quantities dimensionless in the equations of motion. If Equation (2.3) is multiplied by a^4/Dh, it may be written in the following dimensionless form:

$$\frac{\partial^2 u_i}{\partial \tau^2} = \theta \cdot P_i/A_i - \alpha u_i - \beta \frac{\partial u_i}{\partial \tau} - \frac{1}{\lambda^2}[BHO]u_i \, a^4/A_i \qquad (2.8)$$

in which:

$u_i = \frac{w_i}{h}$, dimensionless deflection

$\tau = \frac{t}{T_o}$, dimensionless time

$T_o = (ma^4/D)^{1/2}$, a parameter

$\alpha = ka^4/D$, dimensionless foundation stiffness constant

$\beta = ca^4/DT_o$, dimensionless foundation damping constant

$\theta = a^4/Dh$, a parameter

2.5 Numerical Integration

By the above process, the partial differential equation is reduced to a set of simultaneous ordinary differential equations. In this study these equations are integrated numerically by use of the following formulae (Reference 6):

$$\dot{u}_{i(\tau + \Delta\tau)} = \dot{u}_{i(\tau)} + \frac{\Delta\tau}{2}[\ddot{u}_{i(\tau)} + \ddot{u}_{i(\tau + \Delta\tau)}] \qquad (2.9)$$

$$u_{i(\tau + \Delta\tau)} = u_{i(\tau)} + \Delta\tau \, \dot{u}_{i(\tau)} + \frac{(\Delta\tau)^2}{2} \ddot{u}_{i(\tau)}$$

The dimensionless time increment $\Delta\tau$ used was selected as $1/5\ n^2$ where n is the number of grid divisions. This value corresponds to a time increment equal to a fraction of the smallest period of the plate, which is approximately equal to the fundamental period of a simply supported plate one grid square in size.

2.6 Evaluation of Bending Moments

The deflection of the plate at the node points can be computed as described above. By replacing the space derivatives in the expressions for bending moments by the appropriate finite difference patterns, the moments in the plate can be evaluated.

CHAPTER III

NUMERICAL RESULTS

3.1 General

In this section the method of analysis developed in the preceding chapter is applied to a particular plate, subjected to moving loads. The results obtained are presented in the following pages.

3.1.1 Properties of Plate Considered

The properties of the plate are chosen so as to approximate a concrete slab. The plate used is 10 feet by 10 feet and has a thickness of one foot. It rests on a Winkler type elastic foundation, and is assumed to be in contact with the foundation at all times. The plate is free on all edges. The surface is assumed to be perfectly smooth in a no-load condition. For this study, the plate is divided into an 8 by 8 grid.

The material of the slab is assumed to have the following physical properties: Poisson's ratio-1/4; Young's modulus-2 x 10^6psi; density-1/12 pci.

3.1.2 Definition of Moving Load

The load to be applied to the above plate is an approximation of the wheel load of a highway vehicle or of an aircraft during landing. The load as used consists of a pressure of 35 psi acting over a finite area equal to one grid panel, or 1/64 of the entire plate area. This load moves parallel to an edge of the plate with a constant velocity.

3.1.3 Parameters

The parameters considered in this investigation include: (i) the load velocity; (ii) foundation stiffness; (iii) foundation damping; (iv) load tracking (the distance of the load track to the near parallel edge).

The velocity of the load is varied between 70 and 1000 mph. It is recognized that the upper range of the speeds is too high from the standpoint of current practice. This upper limit was used because the numerical data indicated that dynamic effects did not become conspicuous until the speed exceeded approximately 70 mph. The two intermediate speeds used are 200 and 600 mph. The dimensionless parameter for velocity is $\gamma = vT_o/a$ where v, T_o and a have been defined earlier. The values of γ corresponding to the four velocities, 70, 200, 600, 1000 mph, are .43, 1.21, 3.64, 5.71 respectively.

The stiffness of the foundation is characterized by the stiffness constant k in units of $\#/in/in^2$. In this thesis the value of k used ranges from 150 pci to 800 pci, which approximately covers the practical range of soil and gravel foundations (Reference 10). The dimensionless form of the foundation parameter is $\alpha = ka^4/D$. The value of α corresponding to the four foundation stiffnesses, 150, 250, 614.4, 800 pci, are 101.25, 168.75, 417.72, 540.00 respectively.

Some data, including the effects of foundation damping, were also obtained. The dimensionless parameter for damping is $\beta = ca^4/DT_0$. In this study $\beta = 15$ which corresponds to

about 25% of the critical damping for the first mode if the plate is simply supported.

The tracking of the load is referred to by the first, second, and third track, etc. The first load track represents the edge grid row. The second track refers to the second grid row, etc. Most of the data was taken for a load on the edge or the first load track because, in general, it corresponds to the worst, or governing, case.

3.2 Effects of Load Speed and Foundation Stiffness on Deflections

3.2.1 Response Histories

The response histories of deflections are plotted only for the entry corner and the departure corner (Point 1 and Point 9, respectively, in Figure (2.6)). The greatest deflection of the plate generally occurs at either of these points. The response history of the entry corner is shown in Figure (3.1). In this Figure, the deflections for four velocities and a "static curve" are shown. The static curve was obtained by setting the load velocity $\gamma = .06$ corresponding to 10 mph and the damping parameter $\beta = 15$. All curves are obtained for a foundation stiffness $\alpha = 417.72$, an average to good base. The responses are plotted against the dimensionless time variable:

$$\bar{t} = \frac{t}{(a + \lambda)/v} \qquad (3.1)$$

in which t is time (= 0 when the front of the load touches the plate). Thus $\bar{t}$ represents time scaled by the total time needed by the load to cross the plate. It also denotes the position of the load on the plate; at $\bar{t} = 0.5$, the load is halfway across the plate.

It is seen from the figure that the response curve for $\gamma = 0.43$ oscillates around the static curve with a small amplitude. This indicates that at this speed the response does not differ appreciably from the static load response. As the speed increases the response still oscillates about the static curve, but the amplitude grows larger. It is observed that the largest value of the response occurs at $\gamma = 1.21$. At still higher speeds, the maximum response decreases. At $\gamma = 5.71$, the maximum deflection is below that of the static curve.

As the speed increases the "apparent period" of the oscillations (based on the $\bar{t}$ scale) is seen to increase. This is because $\bar{t}$ is proportional to the load speed (see Equation 3.1). Actually, the periods in terms of time are approximately the same and equal to the fundamental period of the plate. The latter is calculated by considering that the plate vibrates as one unit; that is, every point on the plate would have the same deflection at the same instant. In Table I are presented the period of oscillation for each load speed and the fundamental period for a foundation stiffness $\alpha = 417.72$. Also shown in Table I, for each of the curves in Figure (3.1), is the quantity t_{max} which

denotes the time of maximum response. It is seen that the value of t_{max} decreases with increasing speed.

Figure (3.2) shows, for the same system considered in Figure (3.1), the deflection of Point 9, the departure corner. It is seen that the same general trend exists as in Figure (3.1), except that the largest value of the response now occurs at $\gamma = 3.64$.

3.2.2 Maximum Effects

Each of the preceding curves shows the complete response history for a given load speed. By taking only the maximum response for each speed, a graph such as Figure (3.3) may be constructed. This Figure shows the maximum deflection at Point 1 as a function of the dimensionless velocity parameter γ. Each curve in the Figure represents one foundation stiffness. In general, it is seen that the maximum deflection decreases with speed, as was indicated in the previous section. An exception to this is seen for the two lower curves (stiffer foundations) which "peak" at $\gamma = 1.21$, but then gradually drop as do the others.

As expected, as the foundation stiffness increases, the magnitude of deflections decreases. All the curves appear to be flattening out at greater velocities and approaching some "limiting" deflection, but there is no confirmation of this.

It seems that the response of plates on softer foundations is more sensitive to changes in load speed than are

plates on stiffer foundations. Also, since the spread of points at slower speeds is greater, one could conclude that the response is more sensitive to changes in foundation stiffness at slower speeds. This may be seen also in Figure (3.4) in which the data in Figure (3.3) are replotted using the dimensionless foundation parameter as the abscissa. It is seen that as the speed increases, the curves tend to flatten out. In summary, for Point 1, the maximum response generally decreases with increasing speed. Furthermore, as the speed increases, the effect on response of changes in foundation stiffness decreases.

Similar to the data presented in the preceding two Figures, Figures (3.5) and (3.6) give the maximum deflections for Point 9. In contrast to the trend shown in Figure (3.3), it is seen in Figure (3.5) that the deflection generally increases with speed for speeds up to $\gamma = 3.64$. Beyond that, the value of maximum response decreases, except for the stiffest foundation, $\alpha = 540.00$, at which the deflection at $\gamma = 5.71$ is greater than the value at $\gamma = 3.64$.

It may be noted that the spread of points is approximately the same at all speeds except $\gamma = 5.71$. This would indicate that the foundation does not affect the maximum deflections at Point 9 as greatly as at Point 1.

Figure (3.6) shows the maximum deflection at Point 9 versus the dimensionless foundation parameter α. As the load velocity increases, the slopes of the lines stay about

the same with an exception for the curve $\bar{V}$ = 5.71 which flattens. This would indicate that, except for the $\bar{V}$ = 5.71 speed, the response for all speeds is about equally sensitive to changes in foundation stiffness. At $\bar{V}$ = 5.71 it is less sensitive.

The above presentation has dealt with the entry and departure corners separately. It was found that the maximum deflection of the plate always occurs at either of these two points. In general, the deflection at Point 9 was largest for higher speeds, while that at Point 1 was largest for lower speeds.

3.3 Effects of Load Speed and Foundation Stiffness on Bending Moments

3.3.1 Response Histories

Figure (3.7) shows the time history of the first principal bending moment, M_1, (scaled by a/D to make it dimensionless), for the center point on the loaded edge (Point 5 in Figure (2.6) - the direction of the moment corresponds to that of the load). The foundation used in this Figure is α = 417.72. The static curve is shown, as well as curves for the four load velocities used previously.

It is seen that, irrespective of the load speed, the maximum response occurs at approximately $\bar{t}$ = 0.5, or when the load is at the center of the plate edge. Again, the slower speed deviates only slightly from the static curve. At greater load speeds, the amplitude of the oscillation in-

creases. It is interesting to note the large negative moments. At higher speeds they have the same order of magnitude as the positive moments. At $\gamma = 3.64$ the maximum positive moment is seen to be about 1.5 times the static maximum. At $\gamma = 5.71$, the maximum negative moment is almost numerically equal to the static (positive) maximum.

Shown in Figure (3.8) is the moment history for Point 14 (see Figure (2.6)) which, like Point 5, lies in the middle of the load track, but is one grid length away from the edge. For this point the response curves do not exhibit well defined peaks as observed in the Figure for Point 5. The maximum occurs at $\gamma = 3.64$ and is about 1.67 times the maximum static value. In general, the dynamic effects increase with load speed. This is particularly marked for the $\gamma = 5.71$ curve which shows little relationship to the static curve at the latter part of the passage.

Figure (3.9) shows the moment at Point 23 (see Figure (2.6) which, like Points 5 and 14, lies on the center line of the plate, but is two grid lengths toward the interior of it. This location differs from the preceding two in that the load does not pass directly over it. The response curves are similar to those for Point 14, but the differences with those of Point 5 are even more pronounced here. Thus, at $\bar{t} = 0.5$ the maximum response again occurs for $\gamma = 3.64$, and is now more than twice the static maximum. For the highest load speed, the maximum occurs at $\bar{t} = 0.8$ instead of at 0.5.

From the three preceding figures, it may be concluded that, while the static bending moment decreases at an appreci-

able rate going toward the interior of the plate, the incremental dynamic bending moment, i.e., the difference between maximum dynamic and static moments, tends to stay unchanged. This may be explained by the fact that the natural modes of vibration, excited by the moving load, involve deformation of the entire plate.

Figure (3.10) shows how the foundation stiffness affects the response history of the moment at Point 5. For the speed $\gamma = 5.71$, the bending moment is plotted against $\bar{t}$ for the four foundation stiffnesses. It is seen that the curves are virtually on top of one another for the first 70% of the passage. As indicated by previous data, this portion shows largely the static effect. Since for all foundation stiffnesses the curves almost coincide, this would indicate that for a given speed foundation stiffness has little effect on moments during this stage of the travel. In the latter stages (in which the dynamic effects predominate) however, there is an appreciable difference among the curves for different foundation values. Generally speaking, the dynamic effects are larger for softer foundations.

3.3.2 Maximum Effects

The maximum moments at Point 5 due to different load speeds are plotted in Figure (3.11) for the four values of foundation stiffness. Each value of the foundation stiffness is represented by one line in the Figure. It is seen that at the lowest speed the foundation causes appreciable variations in moment, the softest foundation giving the

largest value. As the load speed increases, the influence of foundation stiffness diminishes; all curves tend to bunch together. The maximum response occurs at $\gamma = 3.64$ for all curves.

The maximum moment at Point 5 as a function of foundation stiffness is shown in Figure (3.12). Here each curve is for one value of load velocity. For the curve $\gamma = .43$, there is a moderate decrease in the value of the maximum moment for increasing foundation stiffness. The other curves appear rather flat, which is simply another way of indicating that at higher speeds the value of the moment is not appreciably affected by foundation stiffness.

Instead of considering the maximum moment at a fixed point as in the above two cases, the maximum moment that has ever occurred in the plate for a given load velocity and foundation stiffness may be considered. This quantity is denoted by the symbol $M_{1,max}$. In Figure (3.13) its dimensionless form is plotted against the speed parameter γ. Again, there is one curve for each value of foundation stiffness. Generally there is an increase in this moment with increasing speed. The softer foundations appear to be levelling off and approaching a single value. The overall values are greater for the softer foundations as would be expected. Beside each plotted point the location where the moment occurred is indicated. As may be seen, the location tends to move toward the departure edge as the load speed increases.

With foundation stiffness as the abscissa, the same data in Figure (3.10) are replotted in Figure (3.14). The flattening of the curves with increasing speed is again evident, indicating a decrease in the influence of foundation stiffness with increasing speed.

3.4 Effects of Damping

The previous results were obtained assuming the foundation to be free from any damping. To obtain some idea about the effect of foundation damping the following data were obtained which included a damping coefficient $\beta = 15$.

3.4.1 Deflections

A typical deflection history curve for Point 1 is shown in Figure (3.15). Comparing this Figure to Figure (3.1), it is apparent that the damping has substantially lessened the dynamic effect. The curve for $\gamma = .43$ now follows the static curve almost exactly. In general, the maximum values were reduced by about 25% from those of the undamped case.

3.4.2 Bending Moments

A typical moment history curve is shown in Figure (3.16) for Point 5. In comparing this with Figure (3.15), a reduction in the dynamic effects is again seen. The curve for $\gamma = .43$ almost coincides with the static one. The maximum values are, in general, reduced by about 25%.

3.5 Effects of Load Tracking

All of the above data were obtained with the load

moving down the first load track, or along an edge of the plate. It was assumed that this would produce greater maximum response in the plate than for the load to move on any of the interior tracks. To verify this assumption, some data were taken with the load moving along the following tracks: the second (between Points 10 and 19); the third (between Points 19 and 28); and the fourth track (between Points 28 and 37). Due to the symmetry of the plate, these tracks cover all possible positions of the load. Two pairs of load speeds and foundation stiffnesses were used in order to cover a reasonable range of dynamic effects. The first set is obtained for γ = .43 and a foundation stiffness α = 417.70. These values were chosen because it was thought they would cause smaller dynamic effects. The second set corresponds to γ = 5.71 and a foundation stiffness of α = 101.25. It was thought that these values would produce the largest dynamic effects.

The response histories of the deflection of Point 1 showed only that the response decreased as the load track moved further from the point. No graphs will be presented for this. The history curves for moment at Point 5 for the load on each of the four tracks is shown in Figure (3.17). As the load track is further away from the point, the sharpness of the peaks of the curve decreases. At the latter part of the passage (for which the dynamic effects predominate) the response could be larger for load at further tracks. However, the differences are small. This, of course, again shows the evenness of the distribution of the dynamic effects.

The data in Figure (3.17) is concerned with the response at a fixed point as the load track changes. Figure (3.18) shows the moment histories for the mid-points on the load tracks, i.e., for the first track - Point 5; for the second track - Point 14; for the third track - Point 13; and for the fourth track - Point 32. It may be seen that the moment for the load on the first track greatly exceeds that for any other case. Thus, the assumption is validated that edge loading represents the most critical case.

CHAPTER IV

SUMMARY OF RESULTS AND CONCLUSIONS

The results obtained in this study are summarized as follows:

1. Position of Load Track--the largest response, for both deflections and bending moments, is obtained when the load moves along an edge of the plate. Therefore, the bulk of the data was obtained for this case.

2. Deflection Behavior--the maximum deflection occurs at either the entry corner or the departure corner. The departure corner generally gives the absolute maximum. The deflection history for this corner shows that the deflection increases with load speed to a point and then decreases at the highest speed considered. The maximum deflection tends to decrease with increasing foundation stiffness.

3. Moment Behavior--the maximum moment occurs at or near the center of the load track, and generally increases with increasing speed. In contrast to the deflection behavior, the moment is not as sensitive to changes in foundation stiffness. At higher load speeds the value of the maximum moment is almost independent of the values of foundation stiffness considered.

4. Foundation Damping--as expected, damping reduces the sharpness of the peaks of response curves as well as the magnitude of the maximum response. The above data were ob-

tained for load speeds in the range of 10 to 1000 mph. As mentioned earlier, the large value for the upper limit was used because it was found that below 70 mph the dynamic effects were quite small.

It should be noted that for this study the intensity of the load is taken to be constant and the pavement surface absolutely smooth. The results presented here would thus indicate that under these conditions the moving load effects are not too significant for speeds currently in use. Usually, however, the surface of the pavement is not absolutely smooth and the load intensity does not remain constant because the load itself is in general a mechanical system with mass and stiffness. A closer approximation to the actual problem would be to consider the dynamic behavior of the load as well as that of the supporting plate. It seems to the author that it is in this direction that future work should be done.

BIBLIOGRAPHY

1. Carlton, P. F. and Behrmann, R. M. "A Model Study of Rigid Pavement Behavior Under Corner and Edge Loading," Proceedings, Highway Research Board, Volume 35, 1956, pp. 139-146.

2. Harr, M. E. "Influence of Vehicle Speed on Pavement Deflections," Proceedings, Highway Research Board, Volume 41, 1962, pp. 77-82.

3. Highway Research Board. "Final Report on Road Test One-MD," Special Report 4, 1952, pp. 121.

4. Leonard, G. A. and Harr, M. E. "Analysis of Concrete Slabs on Ground," Transactions, A.S.C.E., Volume 126, Part 1, 1961, pp. 42-62.

5. Livesley,R. K. "Some Notes on Math Theory of Loaded Elastic Plates Resting on Elastic Foundations," Quarterly Journal of Mechanics and Applied Mathematics, Volume 6, Part 1, March 1953, pp. 32-44.

6. Newmark,N. M. "A Method of Computation for Structural Dynamics," Transactions, A.S.C.E., Volume 127, Part 1, 1962, pp. 1406.

7. Quinn, B. E. and Van Wyk, R. "A Method for Introducing Dynamic Vehicle Loads Into Design of Highways," Proceedings, Highway Research Board, Volume 40, 1961, pp. 111-124.

8. Roesli, et al. "Field Test on a Pre-stressed Concrete Multi-Beam Bridge," Proceedings, Highway Research Board, Volume 35, 1956, pp. 152-171.

9. Sharma, Piyush C. "Dynamic Response of Plates on Elastic Foundation," Ph.D. dissertation, Michigan State University, 1964.

10. Timoshenko, S. and Woinowsky-Kreiger, S. Theory of Plates and Shells, 2nd Edition, New York: McGraw Hill, 1959.

APPENDIX

COMPUTER PROGRAM

A.1 Generation of Equations of Motion

The main problem in generating the equations of motion is the evaluation of the BHO operator at a point. There are six basic BHO patterns as shown in Figure (2.8). Again, these patterns have incorporated the influence of the boundary conditions of the plate. One BHO pattern is taken at a time. Point which are similar in location on the plate, e.g., all corner points, are handled in one sequence, using one particular pattern. To take care of the orientation of the BHO pattern, two variable subscripts, IS and JS, are introduced. These are added to I and J subscripts, such that by changing IS or JS from one to minus one, or vice versa, the orientation of the BHO pattern is changed. For example, for the upper left hand corner, point type one, using BHO pattern 1 (Figure (2.8)), I = 3, J = 3, IS = 1, JS = 1. To treat the upper right hand corner, point type 2, the subscripts are I = 3, J = NC+2, IS = 1, JS = -1. This changes the BHO pattern to include the correct deflection points. The remaining points on the edges adjacent to corners and interior adjacent to the corner are handled in a similar manner using the patterns (2) and (4) of BHO. Points on the edges and adjacent to the edges are handled as above, using patterns (3) and (5). DO loops are used for

points on the same edge. The points in the interior, points type (25), are all handled at once using pattern (6) by a DO loop.

A.2 Input Parameters

Generally, only basic parameters need to be supplied as input to the program. If such quantities as the dimensions of the slab or its physical properties are to be different than the ones used in this thesis, they may be changed by consulting the list of variables in Section A.4.

The foundation stiffness desired is input as the variable SEK. This should be given directly in units of pci and the computer calculates the value of the corresponding dimensionless parameter. The damping parameter is input as the variable SDC, and is likewise converted to dimensionless form by the computer.

The parameters (which have most to do with the "accuracy" of the solution and time required) are the time increment and the grid size. The time increment of numerical integration may be varied by changing TF. The time increment is defined as:

$$\Delta\tau = \frac{1}{TF(NL)^2}$$

so that by changing the Time Factor a larger or smaller time increment is obtained. The number of grid divisions may be varied by changing NL to the desired number of panels.

The parameters of the moving load may be changed to give any desired intensity or load track, as well as any

velocity. The intensity of the load is changed by changing the value of the variable $\overline{P}$ to the desired psi. The velocity of the load must be input in units of inches per seconds. The input velocity is called VEL. It should be noted that because of the way the load is distributed to the mass points it is imperative that the load be positioned exactly over a mass point after an integer number of steps. This being so, the value of d will always range from 0 to λ. Also, this is required for changing the subscripts of the load equations as the load advances over the plate. Since an arbitrarily specified velocity will not necessarily fulfill this requirement, the program computes the number of steps to cross one panel on the basis of input velocity; this variable is NUMSTP in the program. By rounding off to the nearest even step (EVSTEP) the velocity required is found. This is called VELL and is then used throughout the program. The variance between VEL and VELL is a small percent. VELL is printed at the beginning of each output set.

The track of the load is specified by LII. The input value for this must be equal to the smaller of the two index numbers associated with the first pair of node points at which the load enters the plate and between which the load is to travel. For an edge load, LII is one.

A.3 Time Requirement

The time requirement for the program on the CDC 3600 computer of Michigan State University is about 4×10^{-3} sec/degree of freedom/step of integration. The number of degrees of freedom is equal to that of grid points. The

step of integration is equal to the time of crossing divided by the time increment as defined in the numerical integration procedure. For the 8 x 8 grid used herein, the computer times required for $\gamma = .43$ and $\gamma = 1.21$ with $\alpha = 417.72$ are 2 min 50 sec and 2 min 8 sec, respectively.

A.4 List of Fortran Variables

A list of Fortran variables used in the programs and in this appendix is given in the following:

A = d, distance of back of load from last mass point;

AA = α, dimensionless soil elastic constant;

ABAR = distance back of load is from edge of plate;

ACA(I) = assumed acceleration of point (I);

ACD(I) = derived acceleration of point (I);

ACF(I) = final acceleration of point (I);

ANGLE = orientation of the direction of principal moment;

ANG1* = orientation of space-maximum M'_1;

ANG1T = orientation of the maximum M'_1;

B = β, dimensionless soil damping constant;

BEE = $\bar{b}$, distance front of load is from edge, used in load computation;

BETA = parameter of Beta method;

BMX = M'_x, dimensionless bending moment M_x;

BMY = M'_y, dimensionless bending moment M_y;

BMXY = M'_{xy}, dimensionless twisting moment M_{xy};

---

*Number 2 in the suffix similarly will correspond to M'_2.

BMP1 = M'_1, dimensionless principal bending moment;

BMP1MS = space-maximum M_i;

BMP1ST = maximum M'_1;

C = $\frac{n \cdot h}{\lambda}$, factor used in the evaluation of moments;

CLF = conditioning load factor = A_{ij} used in BHO;

D = D, flexural rigidity of plate;

DELTAT = t, real time increment;

DELTAU = $\Delta\tau$, or H;

DPA(I) = assumed deflection of point (I) obtained by using Beta-formula;

DPF(I) = final deflection of point (I);

DPFMS = space maximum deflection at any instant;

DPFST = maximum deflection;

DV = n in floating point;

E = E, modulus of elasticity;

EVSTEP = number of steps of int/grid;

FK = load position parameter;

GRID = NL;

GS = λ, grid size;

H = $\Delta\tau$, time increment in numerical integration;

I, J, K, L, M = variable subscripts;

JUMP = second mass point, used in loading mechanism;

KANCEL = last mass point, used to exit;

LII = load initial point, determines track of travel;

LR = a/b, aspect ratio;

LOCDPF = location of occurrence of maximum deflection;

LOCMP1 = location of occurrence of maximum M'_1;

LOX = load control parameter;

MDS = location of maximum deflection at any instant;

MEVSTEP = fixed form of EVSTEP;

MID = subscript for the center point;

MP1S = location of occurrence of maximum M'_1 at any instant;

MR = number of rows of grid lines;

N = number of first order differential equations;

NB = number of grid divisions on smaller side;

NC = number of columns;

NE = number of second order differential equations and also the number of dependent variables;

NL = n, number of grid divisions on larger side;

NQP = subscript for the quarter point;

NUMSTP = fixed form of TOTSTP;

ONCE = $\nu \times \Delta t$, distance load moves in one step;

PBAR = load intensity in psi;

P(I) = forcing function at a point (I);

PP = printing counter;

PR = ν, Poisson's ratio;

$R_1 = (1 - \nu)^2/2$

$R_2 = -4 + 2\nu + 2\nu^2$

$R_3 = -3 + 2\nu + \nu^2$

$R_4 = 2 - \nu$

$R_5 = -6 + 2\nu$

$R_6 = 2 - 2\nu$

$R_7 = 8 - 4\nu - 3\nu^2$

$R_8 = 7.5 - 4\xi - 2.5\xi^2$;

SIZE = a, length of the longer side of the plate;

STEPS = number of steps/grid based on VEL;

T = θ, constant to be multiplied to p(x,y,t) to make it dimensionless;

TBAR = time/totime = % through load travel;

TDPST = time of occurrence of maximum deflection;

TF = time factor to set $\Delta\tau$;

THICK = h, thickness of plate;

TIME = τ, dimensionless time;

TMP1ST = time of occurrence of maximum M'_1;

TO = T_o, a parameter;

TOLER = tolerance for testing the convergence in Beta method;

TOTIME = total time load takes to cross plate;

TOTSTP = total number of steps in problem;

VEA(I) = assumed velocity of point (I) obtained by using Beta formula;

VEF(I) = final velocity of point (I);

VEL = input velocity;

VELL = velocity used on basis of even number of steps;

WCI = weight per cubic inch of plate;

W(I,J) = u(i,j), dimensionless deflection of point (i,j);

WPR = variable used in peaking section;

WT = m, mass per unit area of plate;

ZIP = GS - VELL * DELTAT, parameter to change base of load equations.

A.5 Fortran Computer Program

```
      PROGRAM LOADRUN
      DIMENSION ACA(625),ACD(625),ACF(625),VEA(625),VEF(625),DPA(625)
     1,DPF(625),W(29,29),BHO(625),P(625)
     1,BMX(625),BMY(625),BMXY(625),ANGLE(625),BMP1(625),BMP2(625)
      COMMON ACA,ACD,ACF,VEA,VEF, DPA,DPF,W,BHO,P,BMX,BMY,BMXY
     1,ANGLE,BMP1,BMP2
C     PLATE SIZE**************************
      LR=1
      SIZE=120.
      THICK=12.
C     *******GRID SIZE*****************
      NL = 8
      NB=NL/LR
      DV=FLOATF(NL)
      GS=SIZE/DV
      C=DV*THICK/GS
      GRID = NL
C     PLATE MATERIAL PROPERTIES**********************
      WCI=144./1728.
      E=2.*10.**6
      PR=.25
      R1=(1.-PR*PR)/2.
      R2=-4.+2.*PR+2.*PR*PR
      R3=-3.+2.*PR+PR*PR
      R4=2.-PR
      R5=-6.+2.*PR
      R6=2.-2.*PR
      R7=8.-4.*PR-3.*PR*PR
      R8=7.5-4.*PR-2.5*PR*PR
C     FOUNDATION MATERIAL AND LOADING PROPERTIES**********************
      READ 292, SEK, VEL, LII
  292 FORMAT(2F10.2,I5)
      SDC=0.
      PBAR = 35.
C     PRINTING COUNTER PARAMETERS ************************
      PP = .005
C     *******BETA METHOD OF INTEGRATION PARAMETERS***********
      BETA=0.
      TOLER=.00000005
      D=(E*THICK**3)/(12.*(1.-PR**2))
      WT=WCI*THICK/386.4
      TF = 5.
      TO=SQRTF((WT*SIZE**4)/D)
      AA=(SEK*SIZE**4)/D
      B=(SDC*SIZE**4)/(D*TO)
      T=(SIZE**4)/(D*THICK)
      DELTAU = 1./(TF*GRID**2)
```

```
      PRINT 696, TF, GRID
  696 FORMAT(1H4,30X,5HTF OF,1X,F5.1,2X,4HAND ,F5.1,2X,9HDIVISIONS/)
      PRINT396, LII,SEK
  396 FORMAT(1H 30X,13HLOAD POSITION,I4,3X,13HFOUNDATION = ,F8.2)
      H = DELTAU
      DELTAT = TO*DELTAU
      STEPS = GS/(VEL*DELTAT)
      EVSTEP = XFIXF(STEPS+0.5)
      VELL = GS/(EVSTEP*DELTAT)
      ONCE = VELL*DELTAT
      TOTSTP = GRID*EVSTEP
      NUMSTP = TOTSTP
      MEVSTP = EVSTEP
      TOTIME = (SIZE + GS)/VELL
      PRINT 205, D, TO, DELTAU, DELTAT
  205 FORMAT(1H0,4HD = ,E17.10/1H ,5HTO = ,E17.10/1H ,9HDELTAU = ,
     1E17.10/1H ,9HDELTAT = ,E17.10)
      PRINT 211, ONCE
  211 FORMAT(1H ,6HONCE =,E17.10)
      PRINT 202, STEPS, EVSTEP,VELL, TOTSTP, NUMSTP
  202 FORMAT(1H , 8HSTEPS = , E17.10/ 1H ,9HEVSTEP = ,E17.10/
     11H ,7HVELL = ,E17.10/1H ,9HTOTSTP = ,E17.10/1H ,9HNUMSTP = , I6/)
      PRINT 424, B
  424 FORMAT(1H ,4HB = ,E17.10)
      TIME = 0
C     EVALUATION OF NUMBER OF ROWS AND COLUMNS,NUMBER OF EQUATIONS ETC
      NC=NL+1
      MR=NB+1
      NE=MR*NC
      MM=MR+2
      NN=NC+2
      MID=NC*NL/2+(NC+1)/2
      MIM=MID-1
      MIP=MID+1
      L = LII
      LOX = 1
      FK = LOX - 1
      NEXT = L + NL - 1
      KANCEL = L + NL
      JUMP = L + 1
      TDPST=0.
      LOCDPF=0.
      DPFST=0.
      TMP1ST=0.
      LOCMP1=0.
      BMP1ST=0.
      TMP2ST=0.
      LOCMP2=0.
      BMP2ST=0.
      ANG1T=0.
      ANG2T=0.
      DO 100 I=1,NE
      ACA(I)=0.
      ACD(I)=0.
```

```
      ACF(I)=0.
      VEA(I)=0.
      VEF(I)=0.
      DPA(I)=0.
      P(I) = 0.
      BMP1(I) = 0
      BMP2(I) = 0
      BMXY(I) = 0
      BMX(I) = 0
      BMY(I) =0
      BHO(I) = 0
      ANGLE(I) = 0
  100 DPF(I)=0.
      DO 969 I = 1,NC
      DO 969 J = 1,MR
  969 W(I,J) = 0
C     BEGIN COMPUTATION OF INITIAL ACCELERATION*****************************
      DO 102 I=1,NE
      ACF(I)=H*H*T*P(I)
  102 ACD(I)=ACF(I)
C     END COMPUTATION OF INITIAL ACCELERATION
  999 TIME = TIME + DELTAT
      TBAR = TIME/TOTIME
  300 DO 301 I=1,NE
      ACA(I)=ACD(I)
      DPA(I)=DPF(I)+VEF(I)+(.5-BETA)*ACF(I)+BETA*ACA(I)
  301 VEA(I)=VEF(I)+.5*(ACF(I)+ACA(I))
C     ************************BEGIN LOAD SELECTION************************
      ABAR = VELL*TIME-GS
      IF(ABAR) 122,103,103
  122 BEE = VELL*TIME
      P(L) = PBAR*BEE*(GS-BEE/2.)/2.
      P(L+1) = PBAR*BEE**2./4.
      P(L + NC) = P(L)
      P(L + NC + 1) = P(L + 1)
      GO TO 106
  103 A = ABAR - FK*GS
      IF(L-NEXT) 104,105,105
  104 P(L) = PBAR*(GS-A)**2./4.
      P(L+1) = PBAR*((GS**2)/2. + A*GS - A**2)/2.
      P(L+2) = PBAR*A**2/4.
      P(L + NC) = P(L)
      P(L + NC + 1) = P(L + 1)
      P(L + NC + 2) = P(L + 2 )
      GO TO 106
  105 P(L) = PBAR*(GS-A)**2/4.
      P(L+1) = PBAR*(GS**2 - A**2)/4.
      P(L + NC) = P(L)
      P(L + NC + 1) = P(L + 1)
  106 IF(L-JUMP) 107, 108, 108
```

```
  108 P(L-1) = 0
      P(L + NL) = 0.
  107 CONTINUE
C     **************************END LOAD SELECTION**************************

C     BEGIN GENERATION OF DIFFERENTIAL EQUATIONS FOR FOR PLATE WITH ALL EDGE
C     FREE*****************************************************************
  368 DO 10 I=3,MM
      DO 10 J=3,NN
      K=(I-3)*NC+J-2
   10 W(I,J)=DPA(K)
C     POINTS AT CORNER ON BOUNDARY(POINTS 1 THRU 4)
      I=3
      J=3
      IS=1
      JS=1
      CF=.25
      CLF = GS**2/4.

      K=(I-3)*NC+J-2
      BHO(K)=R3*(-W(I,J)+W(I,J+JS)+W(I+IS,J))+R1*(W(I,J+2*JS)+W(I+2*IS,J))
     1))+R6*W(I+IS,J+JS)
      ACD(K) = H*H*(T*P(K)/CLF -AA*DPA(K)-BHO(K)*DV**4/CF)-B*H*VEA(K)
      I=3
      J=NC+2
      IS=1
      JS=-1
      K=(I-3)*NC+J-2
      BHO(K)=R3*(-W(I,J)+W(I,J+JS)+W(I+IS,J))+R1*(W(I,J+2*JS)+W(I+2*IS,J))
     1))+R6*W(I+IS,J+JS)
      ACD(K) = H*H*(T*P(K)/CLF -AA*DPA(K)-BHO(K)*DV**4/CF)-B*H*VEA(K)
      I=MR+2
      J=NC+2
      IS=-1
      JS=-1
      K=(I-3)*NC+J-2
      BHO(K)=R3*(-W(I,J)+W(I,J+JS)+W(I+IS,J))+R1*(W(I,J+2*JS)+W(I+2*IS,J))
     1))+R6*W(I+IS,J+JS)
      ACD(K) = H*H*(T*P(K)/CLF -AA*DPA(K)-BHO(K)*DV**4/CF)-B*H*VEA(K)
      I=MR+2
      J=3
      IS=-1
      JS=1
      K=(I-3)*NC+J-2
      BHO(K)=R3*(-W(I,J)+W(I,J+JS)+W(I+IS,J))+R1*(W(I,J+2*JS)+W(I+2*IS,J))
     1))+R6*W(I+IS,J+JS)
      ACD(K) = H*H*(T*P(K)/CLF -AA*DPA(K)-BHO(K)*DV**4/CF)-B*H*VEA(K)
C     POINTS AT INTERIOR CORNER(POINTS 5 THRU 8)
      I=4
      J=4
      IS=1
      JS=1
```

```
      CF=1.
      CLF = GS**2
      K=(I-3)*NC+J-2
      BHO(K)=18.*W(I,J)-8.*(W(I,J+JS)+W(I+IS,J))+2.*W(I+IS,J+JS)
     1+1.*(W(I+2*IS,J)+W(I,J+2*JS))+R4*(W(I-IS,J+JS)+W(I+IS,J-JS))
     1+R5*(W(I-IS,J)+W(I,J-JS))+R6*W(I-IS,J-JS)
      ACD(K) = H*H*(T*P(K)/CLF -AA*DPA(K)-BHO(K)*DV**4/CF)-B*H*VEA(K)
      I=4
      J=NC+1
      IS=1
      JS=-1
      K=(I-3)*NC+J-2
      BHO(K)=18.*W(I,J)-8.*(W(I,J+JS)+W(I+IS,J))+2.*W(I+IS,J+JS)
     1+1.*(W(I+2*IS,J)+W(I,J+2*JS))+R4*(W(I-IS,J+JS)+W(I+IS,J-JS))
     1+R5*(W(I-IS,J)+W(I,J-JS))+R6*W(I-IS,J-JS)
      ACD(K) = H*H*(T*P(K)/CLF -AA*DPA(K)-BHO(K)*DV**4/CF)-B*H*VEA(K)
      I=MR+1
      J=NC+1

      IS=-1
      JS=-1
      K=(I-3)*NC+J-2
      BHO(K)=18.*W(I,J)-8.*(W(I,J+JS)+W(I+IS,J))+2.*W(I+IS,J+JS)
     1+1.*(W(I+2*IS,J)+W(I,J+2*JS))+R4*(W(I-IS,J+JS)+W(I+IS,J-JS))
     1+R5*(W(I-IS,J)+W(I,J-JS))+R6*W(I-IS,J-JS)
      ACD(K) = H*H*(T*P(K)/CLF -AA*DPA(K)-BHO(K)*DV**4/CF)-B*H*VEA(K)
      I=MR+1
      J=4
      IS=-1
      JS=1
      K=(I-3)*NC+J-2
      BHO(K)=18.*W(I,J)-8.*(W(I,J+JS)+W(I+IS,J))+2.*W(I+IS,J+JS)
     1+1.*(W(I+2*IS,J)+W(I,J+2*JS))+R4*(W(I-IS,J+JS)+W(I+IS,J-JS))
     1+R5*(W(I-IS,J)+W(I,J-JS))+R6*W(I-IS,J-JS)
      ACD(K) = H*H*(T*P(K)/CLF -AA*DPA(K)-BHO(K)*DV**4/CF)-B*H*VEA(K)
C     POINTS ON BOUNDARY ADJACENT TO CORNERS(POINTS9 THRU 16)
C     ROWS(POINTS 9,10,11,12)
      I=3
      J=4
      IS=1
      JS=1
      CF=.5
      CLF = GS**2/2.
      K=(I-3)*NC+J-2
      BHO(K)=R8*W(I,J)+R3*W(I,J-JS)+R2*W(I,J+JS)+R1*W(I,J+2*JS)
     1+R4*(W(I+IS,J-JS)+W(I+IS,J+JS))+R5*W(I+IS,J)+W(I+2*IS,J)
      ACD(K) = H*H*(T*P(K)/CLF -AA*DPA(K)-BHO(K)*DV**4/CF)-B*H*VEA(K)
      I=3
      J=NC+1
      IS=1
      JS=-1
```

```
      K=(I-3)*NC+J-2
      BHO(K)=R8*W(I,J)+R3*W(I,J-JS)+R2*W(I,J+JS)+R1*W(I,J+2*JS)
     1+R4*(W(I+IS,J-JS)+W(I+IS,J+JS))+R5*W(I+IS,J)+W(I+2*IS,J)
      ACD(K) = H*H*(T*P(K)/CLF -AA*DPA(K)-BHO(K)*DV**4/CF)-B*H*VEA(K)
      I=MR+2
      J=NC+1
      IS=-1
      JS=-1
      K=(I-3)*NC+J-2
      BHO(K)=R8*W(I,J)+R3*W(I,J-JS)+R2*W(I,J+JS)+R1*W(I,J+2*JS)
     1+R4*(W(I+IS,J-JS)+W(I+IS,J+JS))+R5*W(I+IS,J)+W(I+2*IS,J)
      ACD(K) = H*H*(T*P(K)/CLF -AA*DPA(K)-BHO(K)*DV**4/CF)-B*H*VEA(K)
      I=MR+2
      J=4
      IS=-1
      JS=1
      K=(I-3)*NC+J-2
      BHO(K)=R8*W(I,J)+R3*W(I,J-JS)+R2*W(I,J+JS)+R1*W(I,J+2*JS)
     1+R4*(W(I+IS,J-JS)+W(I+IS,J+JS))+R5*W(I+IS,J)+W(I+2*IS,J)
      ACD(K) = H*H*(T*P(K)/CLF -AA*DPA(K)-BHO(K)*DV**4/CF)-B*H*VEA(K)
C     COLUMNS((POINTS 13,14,15,16)
      I=4
      J=3
      IS=1
      JS=1
      K=(I-3)*NC+J-2
      BHO(K)=R8*W(I,J)+R3*W(I-IS,J)+R1*W(I+2*IS,J)+R4*(W(I-IS,J+JS)
     1+W(I+IS,J+JS))+R5*W(I,J+JS)+W(I,J+2*JS)+R2*W(I+IS,J)
      ACD(K) = H*H*(T*P(K)/CLF -AA*DPA(K)-BHO(K)*DV**4/CF)-B*H*VEA(K)
      I=4
      J=NC+2
      K=(I-3)*NC+J-2
      IS=1
      JS=-1
      BHO(K)=R8*W(I,J)+R3*W(I-IS,J)+R1*W(I+2*IS,J)+R4*(W(I-IS,J+JS)
     1+W(I+IS,J+JS))+R5*W(I,J+JS)+W(I,J+2*JS)+R2*W(I+IS,J)
      ACD(K) = H*H*(T*P(K)/CLF -AA*DPA(K)-BHO(K)*DV**4/CF)-B*H*VEA(K)
      I=MR+1
      J=NC+2
      IS=-1
      JS=-1
      K=(I-3)*NC+J-2
      BHO(K)=R8*W(I,J)+R3*W(I-IS,J)+R1*W(I+2*IS,J)+R4*(W(I-IS,J+JS)
     1+W(I+IS,J+JS))+R5*W(I,J+JS)+W(I,J+2*JS)+R2*W(I+IS,J)
      ACD(K) = H*H*(T*P(K)/CLF -AA*DPA(K)-BHO(K)*DV**4/CF)-B*H*VEA(K)
      I=MR+1
      J=3
      IS=-1
      JS=1
      K=(I-3)*NC+J-2
      BHO(K)=R8*W(I,J)+R3*W(I-IS,J)+R1*W(I+2*IS,J)+R4*(W(I-IS,J+JS)
     1+W(I+IS,J+JS))+R5*W(I,J+JS)+W(I,J+2*JS)+R2*W(I+IS,J)
      ACD(K) = H*H*(T*P(K)/CLF -AA*DPA(K)-BHO(K)*DV**4/CF)-B*H*VEA(K)
```

```
C       POINTS ON THE BOUNDARY THIRD FROM CORNERS
C       TOP ROW(POINTS TYPE 17)
        I=3
        IS=1
        CF=.5
        DO 12 J=5,NC
        K=(I-3)*NC+J-2
        BHO(K)=R7*W(I,J)+R2*(W(I,J-1)+W(I,J+1))+R1*(W(I,J-2)+W(I,J+2))
       1+R4*(W(I+IS,J-1)+W(I+IS,J+1))+R5*W(I+IS,J)+W(I+2*IS,J)
   12 ACD(K) = H*H*(T*P(K)/CLF -AA*DPA(K)-BHO(K)*DV**4/CF)-B*H*VEA(K)
C       BOTTOM ROW(POINTS TYPE 18)
        I=MR+2
        IS=-1
        DO 13 J=5,NC
        K=(I-3)*NC+J-2
        BHO(K)=R7*W(I,J)+R2*(W(I,J-1)+W(I,J+1))+R1*(W(I,J-2)+W(I,J+2))
       1+R4*(W(I+IS,J-1)+W(I+IS,J+1))+R5*W(I+IS,J)+W(I+2*IS,J)
   13 ACD(K) = H*H*(T*P(K)/CLF -AA*DPA(K)-BHO(K)*DV**4/CF)-B*H*VEA(K)
C       LEFT COLUMN BOUNDARY(POINTS TYPE 19)
        J=3
        JS=1
        DO 14 I=5,MR
        K=(I-3)*NC+J-2
        BHO(K)=R7*W(I,J)+R2*(W(I-1,J)+W(I+1,J))+R1*(W(I-2,J)+W(I+2,J))
       1+R4*(W(I-1,J+JS)+W(I+1,J+JS))+R5*W(I,J+JS)+W(I,J+2*JS)
   14 ACD(K) = H*H*(T*P(K)/CLF -AA*DPA(K)-BHO(K)*DV**4/CF)-B*H*VEA(K)
C       RIGHT COLUMN BOUNDARY(POINTS TYPE 20)
        J=NC+2
        JS=-1
        DO 15 I=5,MR
        K=(I-3)*NC+J-2
        BHO(K)=R7*W(I,J)+R2*(W(I-1,J)+W(I+1,J))+R1*(W(I-2,J)+W(I+2,J))
       1+R4*(W(I-1,J+JS)+W(I+1,J+JS))+R5*W(I,J+JS)+W(I,J+2*JS)
   15 ACD(K) = H*H*(T*P(K)/CLF -AA*DPA(K)-BHO(K)*DV**4/CF)-B*H*VEA(K)
C       POINTS INTERIOR AND ADJACENT TO BOUNDARY
C       TOP ROW(POINTS TYPE 21)
        I=4
        IS=1
        CF=1.
        CLF = GS**2

        DO 16 J=5,NC
        K=(I-3)*NC+J-2
        BHO(K)=19.*W(I,J)-8.*(W(I,J-1)+W(I,J+1)+W(I+IS,J))+2.*(W(I+IS,J-1)
       1+W(I+IS,J+1))+W(I+2*IS,J)+R4*(W(I-IS,J-1)+W(I-IS,J+1))+R5*W(I-IS,J
       1)+W(I,J+2)+W(I,J-2)
   16 ACD(K) = H*H*(T*P(K)/CLF -AA*DPA(K)-BHO(K)*DV**4/CF)-B*H*VEA(K)
C       BOTTOM ROW(POINTS TYPE 22)
        I=MR+1
        IS=-1
```

```
      DO 17 J=5,NC
      K=(I-3)*NC+J-2
      BHO(K)=19.*W(I,J)-8.*(W(I,J-1)+W(I,J+1)+W(I+IS,J))+2.*(W(I+IS,J-1)
     1+W(I+IS,-+1))+W(I+2*IS,J)+R4*(W(I-IS,J-1)+W(I-IS,J+1))+R5*W(I-IS,J
     1)+W(I,J+2)+W(I,J-2)
   17 ACD(K) = H*H*(T*P(K)/CLF -AA*DPA(K)-BHO(K)*DV**4/CF)-B*H*VEA(K)
C     LEFT COLUMN(POINTS TYPE 23)
      J=4
      JS=1
      DO 18 I=5,MR
      K=(I-3)*NC+J-2
      BHO(K)=19.*W(I,J)-8.*(W(I-1,J)+W(I+1,J)+W(I,J+JS))+2.*(W(I-1,J+JS)
     1+W(I+1,J+JS))+W(I,J+2*JS)+R4*(W(I-1,J-JS)+W(I+1,J-JS))+R5*W(I,J-JS
     1)+W(I-2,-)+W(I+2,J)
   18 ACD(K) = H*H*(T*P(K)/CLF -AA*DPA(K)-BHO(K)*DV**4/CF)-B*H*VEA(K)
C     RIGHT COLUMN(POINTS TYPE 24)
      J=NC+1
      JS=-1
      DO 19 I=5,NC
      K=(I-3)*NC+J-2
      BHO(K)=19.*W(I,J)-8.*(W(I-1,J)+W(I+1,J)+W(I,J+JS))+2.*(W(I-1,J+JS)
     1+W(I+1,J+JS))+W(I,J+2*JS)+R4*(W(I-1,J-JS)+W(I+1,J-JS))+R5*W(I,J-JS
     1)+W(I-2,J)+W(I+2,J)
   19 ACD(K) = H*H*(T*P(K)/CLF -AA*DPA(K)-BHO(K)*DV**4/CF)-B*H*VEA(K)
C     POINTS IN THE INTERIOR(5,5),(5,N),(M,5),(M,N)
C     POINTS TYPE 25.
      CF=1.
      DO 20 I=5,MR
      DO 20 J=5,NC
      K=(I-3)*NC+J-2
      BHO(K)=20.*W(I,J)-8.*(W(I,J-1)+W(I,J+1)+W(I-1,J)+W(I+1,J))
     1+2.*(W(I-1,J-1)+W(I-1,J+1)+W(I+1,J-1)+W(I+1, J+1))
     2+W(I-2,J)+W(I+2,J)+W(I,J-2)+W(I,J+2)
   20 ACD(K) = H*H*(T*P(K)/CLF -AA*DPA(K)-BHO(K)*DV**4/CF)-B*H*VEA(K)
C     END GENERATION OF EQUATIONS**************************************
C     TEST CONVERGENCE*****************
      MARK=0
      DO 500 I=1,NE
      ERROR=ABSF(ACD(I)-ACA(I))
      IF(ERROR-TOLER)500,500,600
  600 MARK=1
  500 CONTINUE
      IF(MARK)800,800,300
  800 DO 801 I=1,NE
      ACF(I)=ACD(I)
      VEF(I)=VEA(I)
  801 DPF(I)=DPA(I)
C     **************COMPUTE MOMENTS*********************************
      DO 601 I=3,MM
      DO 601 J=3,NN
      K=(I-3)*(NN-2)+J-2
  601 W(I,J)=DPF(K)
```

```
      MMM=MM-1
      NNN=NN-1
      DO 602 I=4,MMM
      DO 602 J=4,NNN
      K=(I-3)*(NN-2)+J-2
      BMX(K)=-C*(-(2.+2.*PR)*W(I,J)+W(I,J-1)+W(I,J+1)+PR*(W(I-1,J)+W(
     1I+1,J)))
      BMY(K)=-C*(-(2.+2.*PR)*W(I,J)+W(I-1,J)+W(I+1,J)+PR*(W(I,J-1)+W(I,J
     1+1)))
  602 BMXY(K)=C*(1.-PR)*(W(I-1,J-1)+W(I+1,J+1)-W(I+1,J-1)-W(I-1,J+1))/4.
C     TOP ROW*****************************
      I=3
      IS=1
      DO 603 J=4,NNN
      K=(I-3)*NC+J-2
      BMX(K)=-C*(W(I,J-1)-2.*W(I,J)+W(I,J+1)+PR*(2.*W(I,J)-5.*W(I+IS,J)
     1+4.*W(I+2*IS,J)-W(I+3*IS,J)))
      BMY(K)=0.
  603 BMXY(K)=0.
C     BOTTOM ROW**************************
      I=MM
      IS=-1
      DO 604 J=4,NNN
      K=(I-3)*NC+J-2
      BMX(K)=-C*(W(I,J-1)-2.*W(I,J)+W(I,J+1)+PR*(2.*W(I,J)-5.*W(I+IS,J)
     1+4.*W(I+2*IS,J)-W(I+3*IS,J)))
      BMY(K)=0.
  604 BMXY(K)=0.
C     LEFT HAND COLUMN********************
      J=3
      JS=1
      DO 605 I=4,MMM
      K=(I-3)*NC+J-2
      BMX(K)=0.
      BMY(K)=-C*(W(I-1,J)-2.*W(I,J)+W(I+1,J)+PR*(2.*W(I,J)-5.*W(I,J+JS)
     1+4.*W(I,J+2*JS)-W(I,J+3*JS)))
  605 BMXY(K)=0.
C     RIGHT HAND COLUMN
      J=NN
      JS=-1
      DO 606 I=4,MMM
      K=(I-3)*NC+J-2
      BMX(K)=0.
      BMY(K)=-C*(W(I-1,J)-2.*W(I,J)+W(I+1,J)+PR*(2.*W(I,J)-5.*W(I,J+JS)
     1+4.*W(I,J+2*JS)-W(I,J+3*JS)))
  606 BMXY(K)=0.
      NEM = NE - 1
      DO 607 I = 2,NEM
  663 IF(BMX(I)-BMY(I)) 664,607,664
  664 ANGLE(I)=ATANF(2.*BMXY(I)/(BMX(I)-BMY(I)))*.5*57.2958
      BMP1(I)=(BMX(I)+BMY(I))*.5+SQRTF(((BMX(I)-BMY(I))*.5)**2+BMXY(I)**
     12)
```

```
      BMP2(I)=(BMX(I)+BMY(I))*.5-SQRTF(((BMX(I)-BMY(I))*.5)**2+BMXY(I)**
     12)
  607 CONTINUE
C     END MOMENT EVALUATION**********************
C     BEGIN MAXIMUM QUANTITIES EVALUATION IN SPACE**********************
      BMP1MS=0.
      BMP2MS=0.
      DPFMS=0.
      DO 608 I=1,NE
      IF(ABSF(BMP1(I))-ABSF(BMP1MS))608,608,609
  609 BMP1MS=BMP1(I)
      ANG1=ANGLE(I)
      MP1S=I
  608 CONTINUE
      DO 700 I=1,NE
      IF(ABSF(BMP2(I))-ABSF(BMP2MS))700,700,701
  701 BMP2MS=BMP2(I)
      ANG2=ANGLE(I)

      MP2S=I
  700 CONTINUE
      DO 702 I=1,NE
      IF(ABSF(DPF(I))-ABSF(DPFMS))702,702,703
  703 DPFMS=DPF(I)
      MDS=I
  702 CONTINUE
C     ENDIN MAXIMUM QUANTITIES EVALUATION**********************************
C     BEGIN MAXIMUM QUANTITIES EVALUATION IN TIME**********************
      IF(ABSF(BMP1MS) -ABSF(BMP1ST))704,704,705
  705 BMP1ST=BMP1MS
      LOCMP1=MP1S
      ANG1T=ANG1
      TMP1ST=TIME
  704 IF(ABSF(BMP2MS) -ABSF(BMP2ST))706,706,707
  707 BMP2ST=BMP2MS
      LOCMP2=MP2S
      ANG2T=ANG2
      TMP2ST=TIME
  706 IF(ABSF(DPFMS)-ABSF(DPFST))708,708,709
  709 DPFST=DPFMS
      LOCDPF=MDS
      TDPST=TIME
  708 CONTINUE
C     END MAX EVALUATION IN TIME**********************************************
      IF(TBAR-PP) 802,803,803
  803 CONTINUE
      PRINT 8031, TIME, TBAR
 8031 FORMAT(1H0,55X,7HTIME = ,F11.7,4X,7HTBAR = ,E17.10)
      PRINT 888, ABAR
  888 FORMAT (1H ,7HABAR = ,E11.4)
```

```
      PRINT 804,MDS,DPFMS,MP1S,BMP1MS,MP2S,BMP2MS
804   FORMAT(1H ,4HMDS=,I3,3X,6HDPFMS=,F11.7,3X,5HMP1S=,I3,3X,7HBMP1MS=,
     1F11.7,3X,5HMP2S=,I3,3X,7HBMP2MS=,F11.7)
      PRINT 8044,ANG1,ANG2
8044  FORMAT(1H ,5HANG1=,F7.3,5X,5HANG2=,F7.3)
      PRINT 761
 761  FORMAT(1H ,4HBMP1)
      PRINT 762, (BMP1(I),I = 1,45)
 762  FORMAT(1H ,9(F11.7,1X))
      PRINT 763
 763  FORMAT(1H ,4HBMP2)
      PRINT 764,(BMP2(I), I = 1,45)
 764  FORMAT(1H , 9(F11.7,1X))
      PRINT 765, DPF(1), DPF(9),DPF(21),DPF(26),DPF(41)
 765  FORMAT(1H ,9HDPF(1) = ,F11.7,3X,9HDPF(9) = , F11.7,3X,
     110HDPF(21) = ,F11.7,3X,10HDPF(26) = ,F11.7,3X,10HDPF(41) = ,
     2F11.7)
      PP = PP + .005
 802  CONTINUE
 113  IF(ABAR) 999, 115, 115
 115  ZIP = GS - VELL*DELTAT
 116  IF(A - ZIP) 118, 117, 117
 117  L = L + 1
      LOX = LOX + 1
      FK = LOX - 1
 118  IF(L - KANCEL) 999,364,364
 364  DO 365 MOP = 1,NE
      P(MOP) = 0.
 365  CONTINUE
      WPR = DPF(9) +2.*10.**(-4)
      IF(WPR - DPFST) 119,366,366
 366  TIME = TIME + DELTAT
      TBAR = TIME/TOTIME
      DO 367 I=1,NE
      ACA(I)=ACD(I)
      DPA(I)=DPF(I)+VEF(I)+(.5-BETA)*ACF(I)+BETA*ACA(I)
 367  VEA(I)=VEF(I)+.5*(ACF(I)+ACA(I))
      GO  TO 368
 119  CONTINUE
      PRINT 8050,TDPST,LOCDPF,DPFST
8050  FORMAT(1H0,6HTDPST=,F9.7,3X,7HLOCDPF=,I3,3X,6HDPFST=,F11.7)
      PRINT 8051,TMP1ST,LOCMP1,BMP1ST
8051  FORMAT(1H ,7HTMP1ST=,F9.7,3X,7HLOCMP1=,I3,3X,7HBMP1ST=,F11.7)
      PRINT 8052,TMP2ST,LOCMP2,BMP2ST
8052  FORMAT(1H ,7HTMP2ST=,F9.7,3X,7HLOCMP2=,I3,3X,7HBMP2ST=,F11.7)
      PRINT 8053,ANG1T,ANG2T
8053  FORMAT(1H ,6HANG1T=,F7.3,5X,6HANG2T=,F7.3)
1000  CONTINUE
1001  CONTINUE
      END
```

TABLE I

PERIOD OF OSCILLATION AND t_{max} FOR k = 614.4 pci

Load Speed (mph)	Period (Seconds)	t_{max} (Seconds)
70	.011	.012660
200	.014	.006661
600	.013	.004441
1000	.015	.003788
Fundamental Period	.0129	

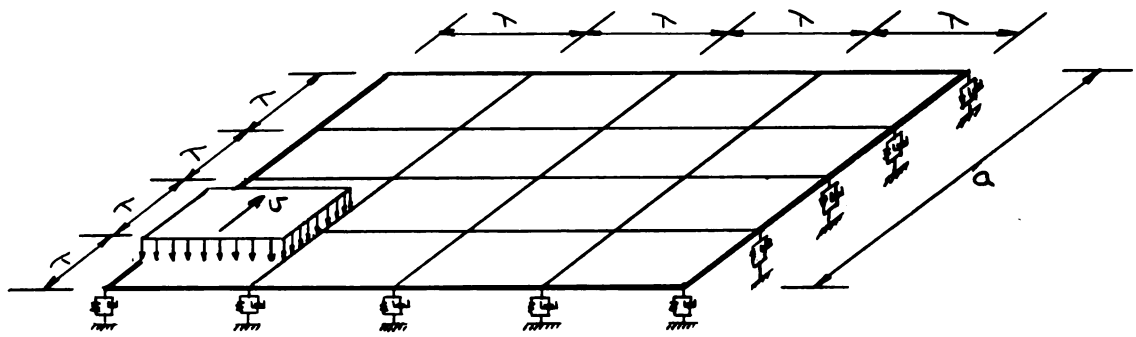

FIG. 2.1 SCHEMATIC DIAGRAM OF SYSTEM CONSIDERED.

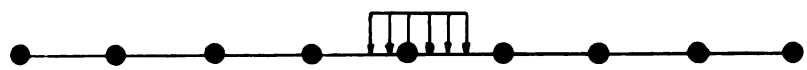

FIG. 2.2 DISTRIBUTED LINE LOAD LUMPED FROM ORIGINAL LOADING.

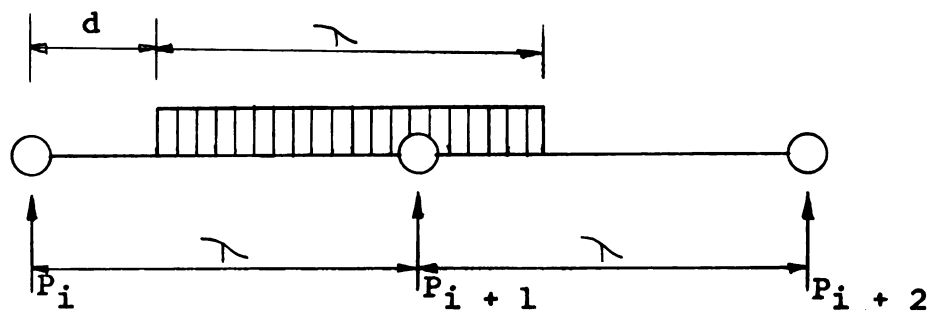

FIG. 2.3 SIMPLE BEAM REACTIONS TO BE USED AS CONCENTRATED LOADS.

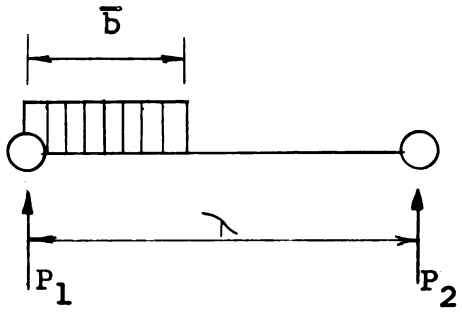

FIG. 2.4 LOAD ENTERING PLATE.

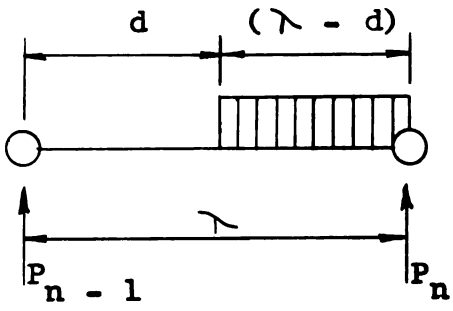

FIG. 2.5 LOAD LEAVING PLATE.

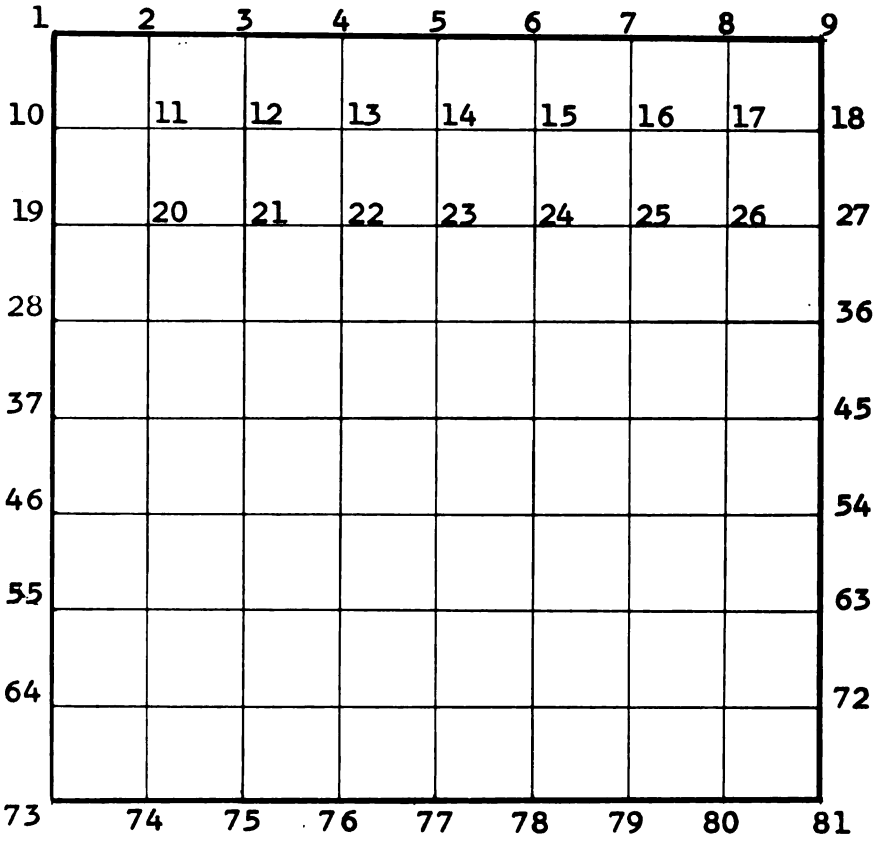

FIG. 2.6 NUMBERING OF NODE POINTS

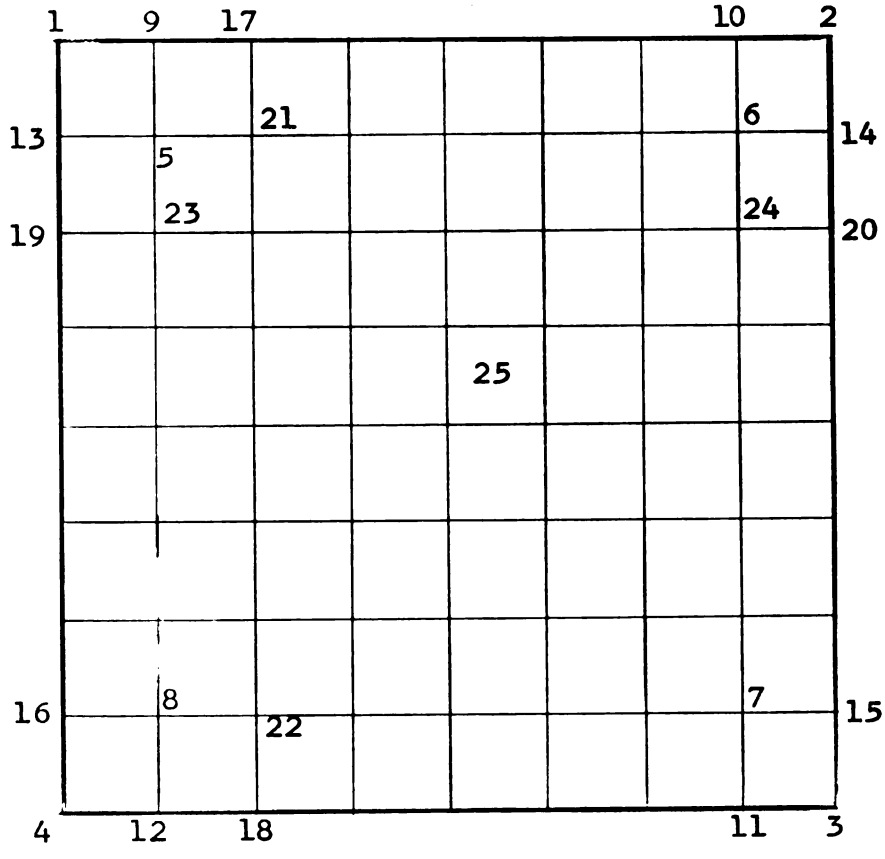

FIG. 2.7 "TYPE" NUMBERING OF NODE POINTS.

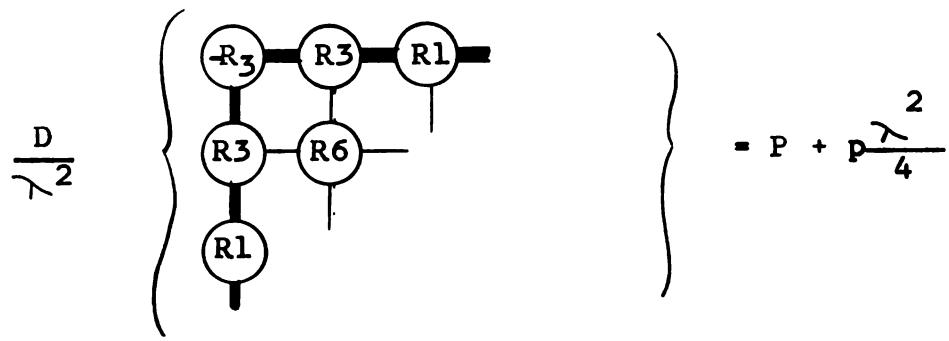

- 1 -

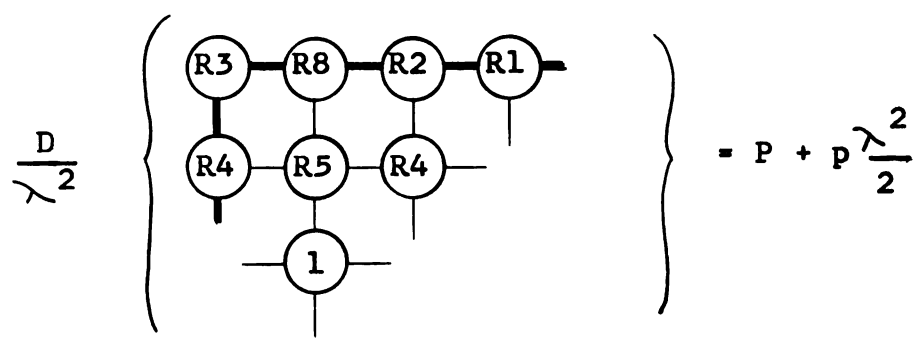

- 2 -

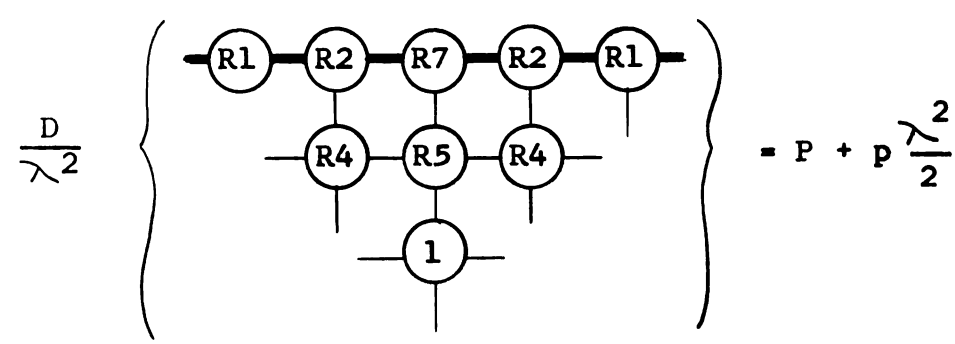

- 3 -

FIG. 2.8 BHO PATTERNS

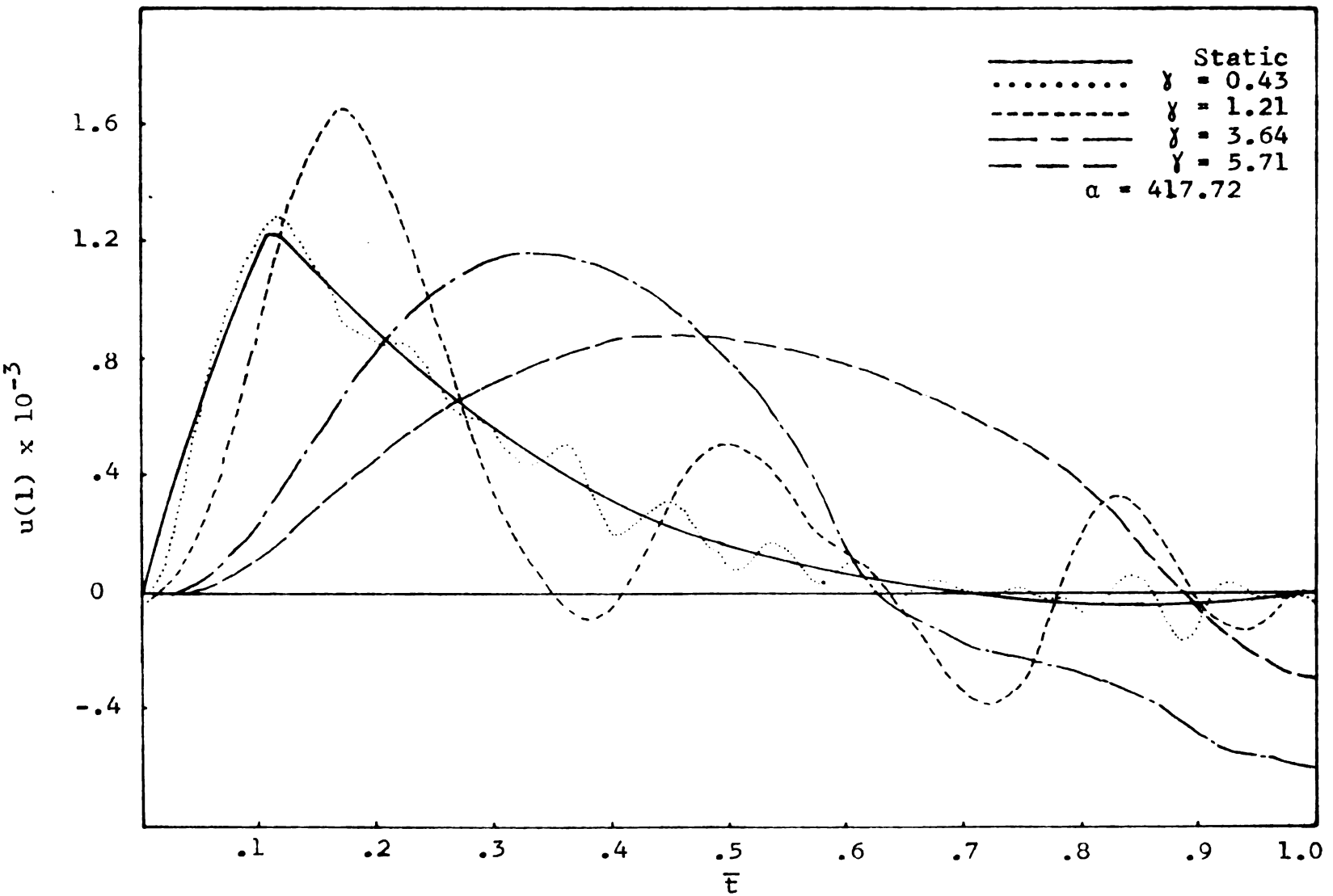

Fig. 3.1 DEFLECTION HISTORY CURVES FOR ENTRY CORNER FOR VARIOUS VELOCITIES.

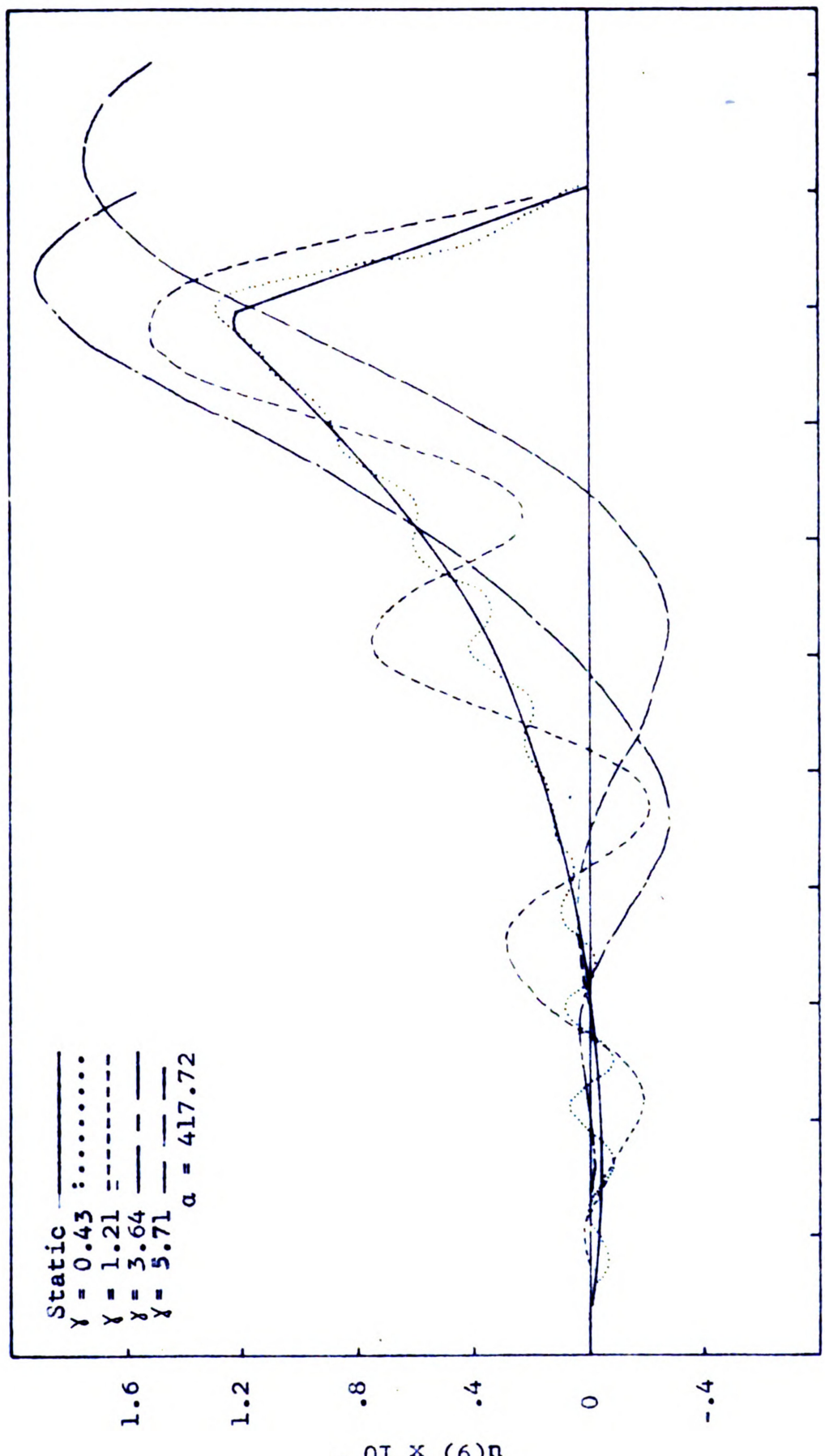

Fig. 3.2 DEFLECTION HISTORY CURVES FOR DEPARTURE CORNER FOR VARIOUS VELOCITIES

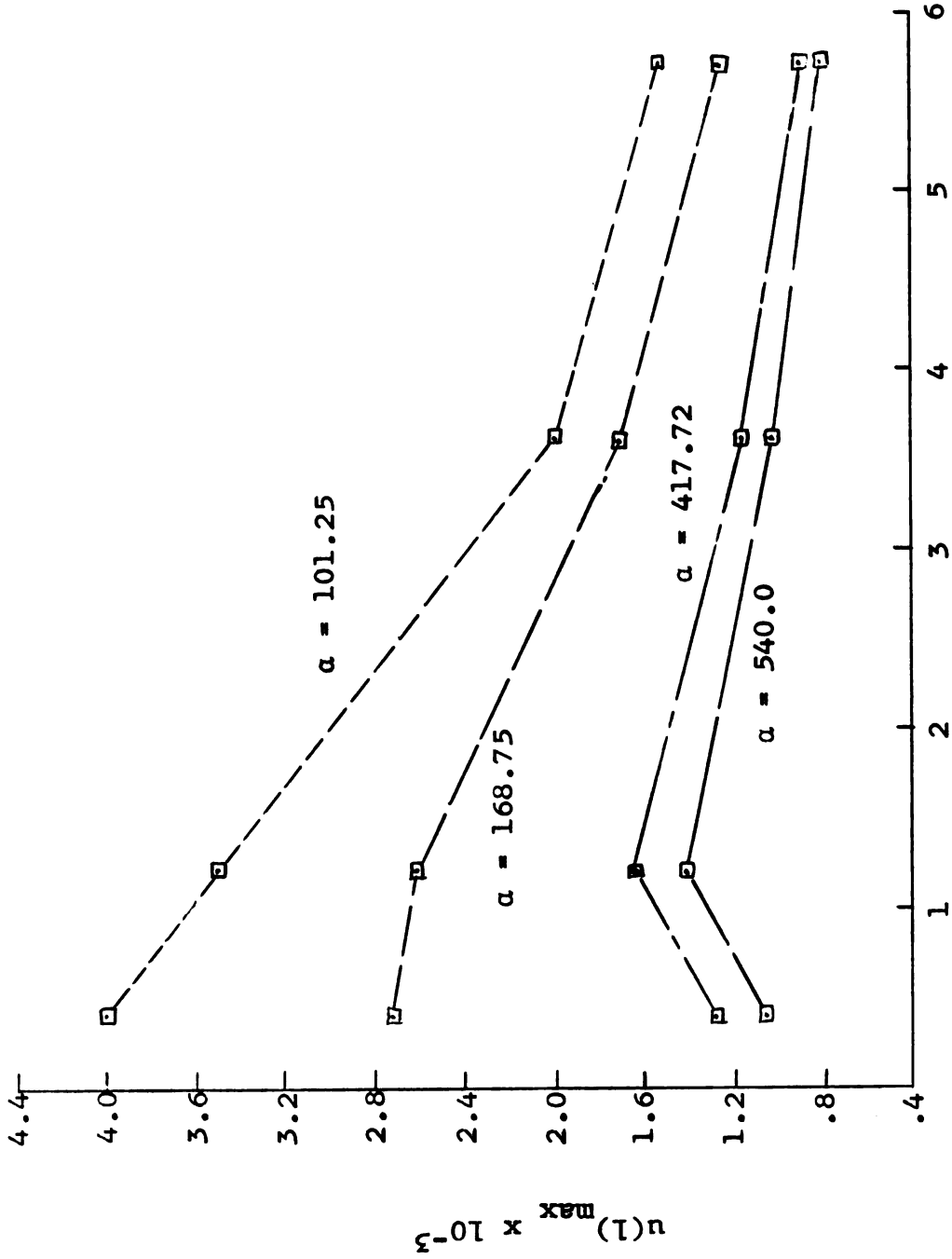

FIG. 3.3 MAXIMUM DISPLACEMENT OF ENTRY CORNER VERSUS LOAD VELOCITY.

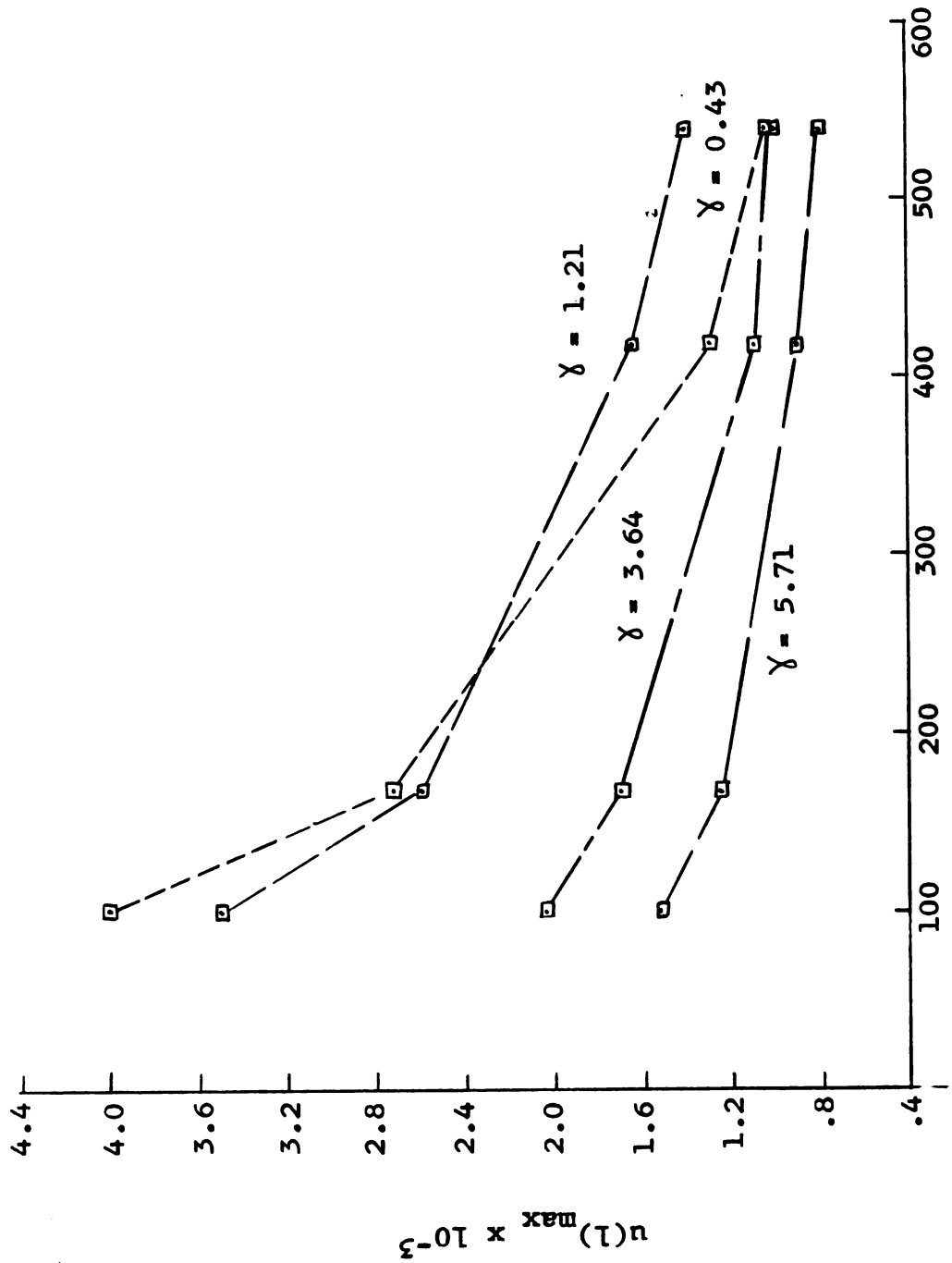

FIG. 3.4 MAXIMUM DISPLACEMENT OF ENTRY CORNER VERSUS FOUNDATION STIFFNESS.

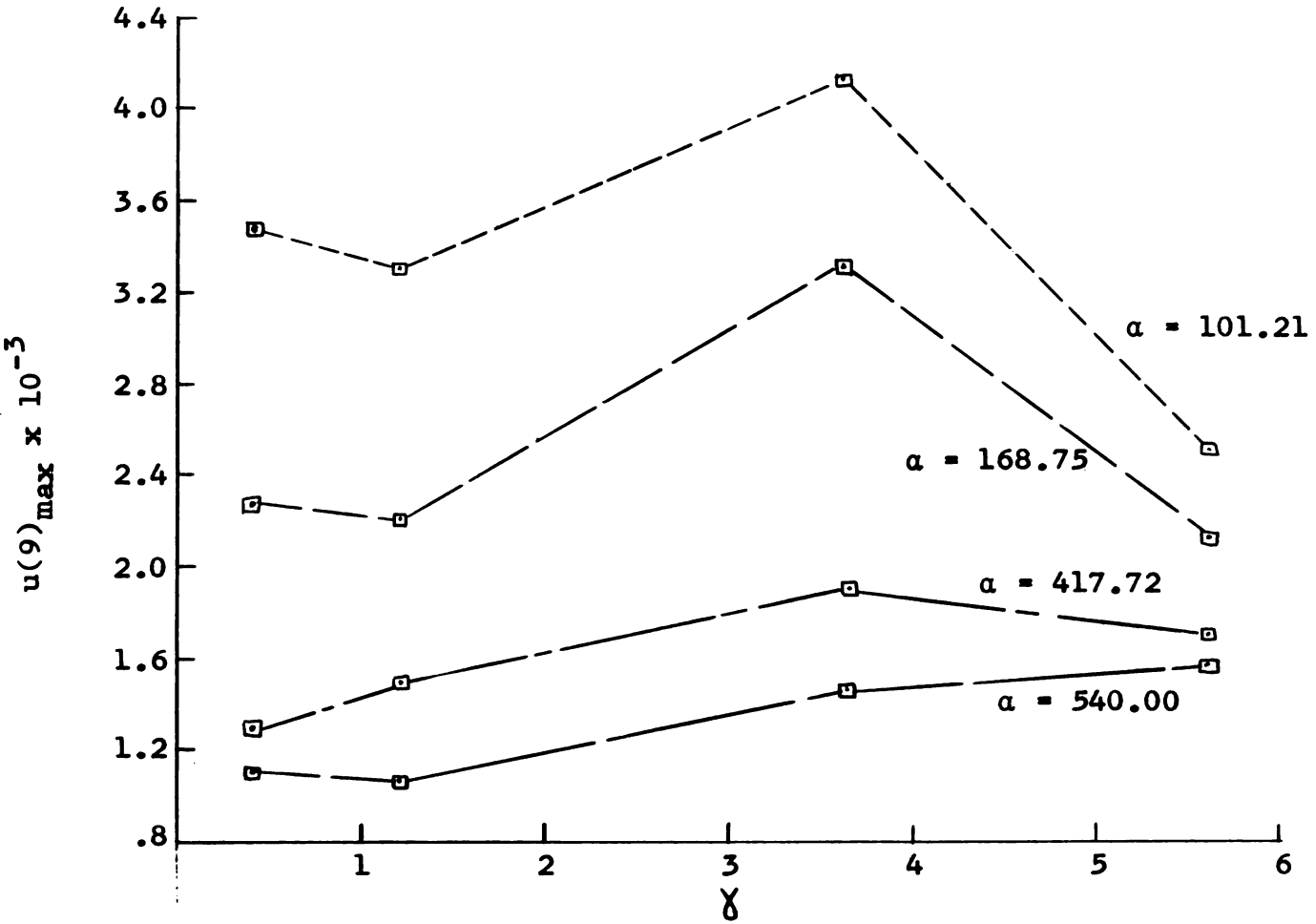

FIG. 3.5 MAXIMUM DISPLACEMENT OF DEPARTURE CORNER VERSUS LOAD VELOCITY.

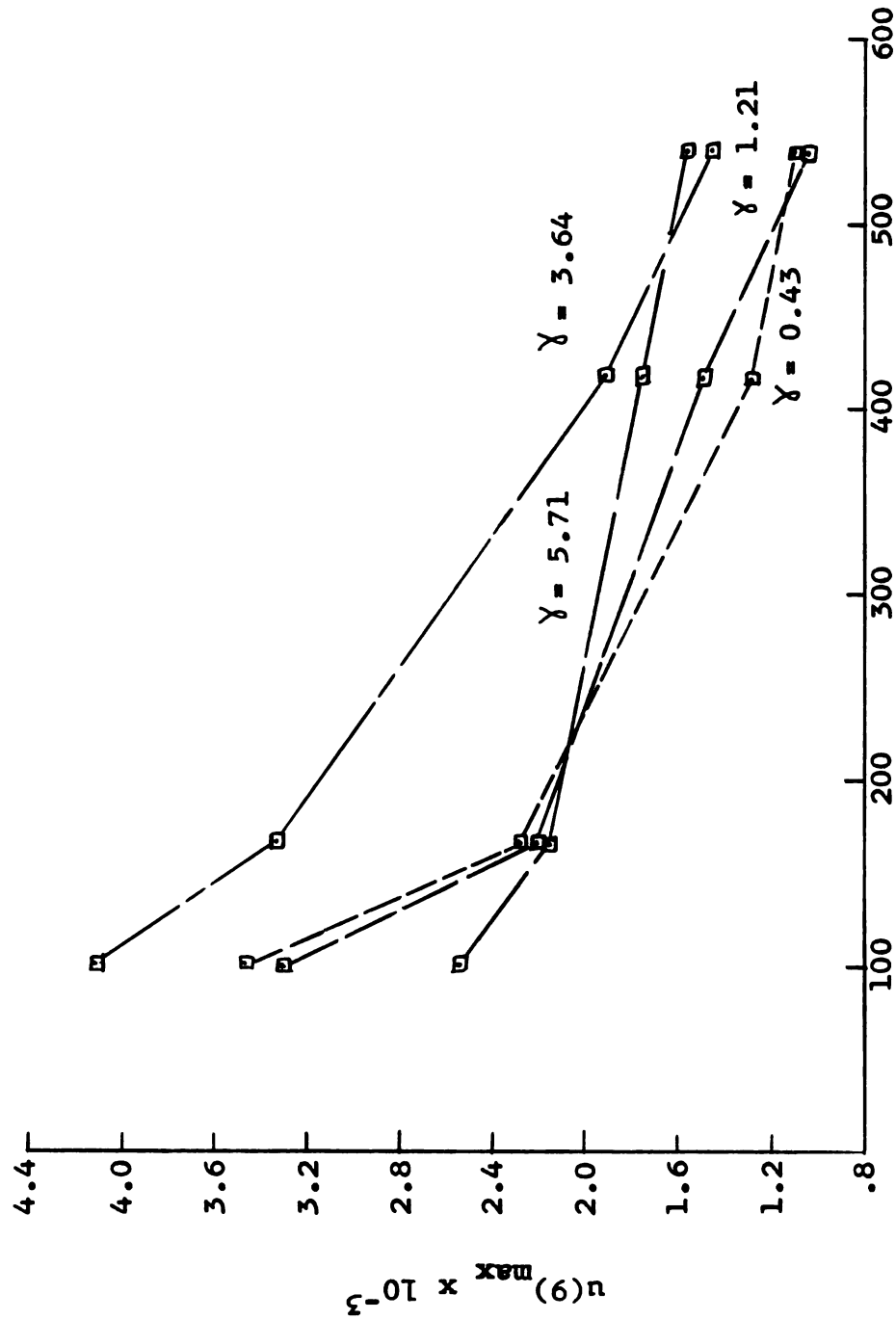

FIG. 3.6 MAXIMUM DISPLACEMENT OF DEPARTURE CORNER VERSUS FOUNDATION STIFFNESS.

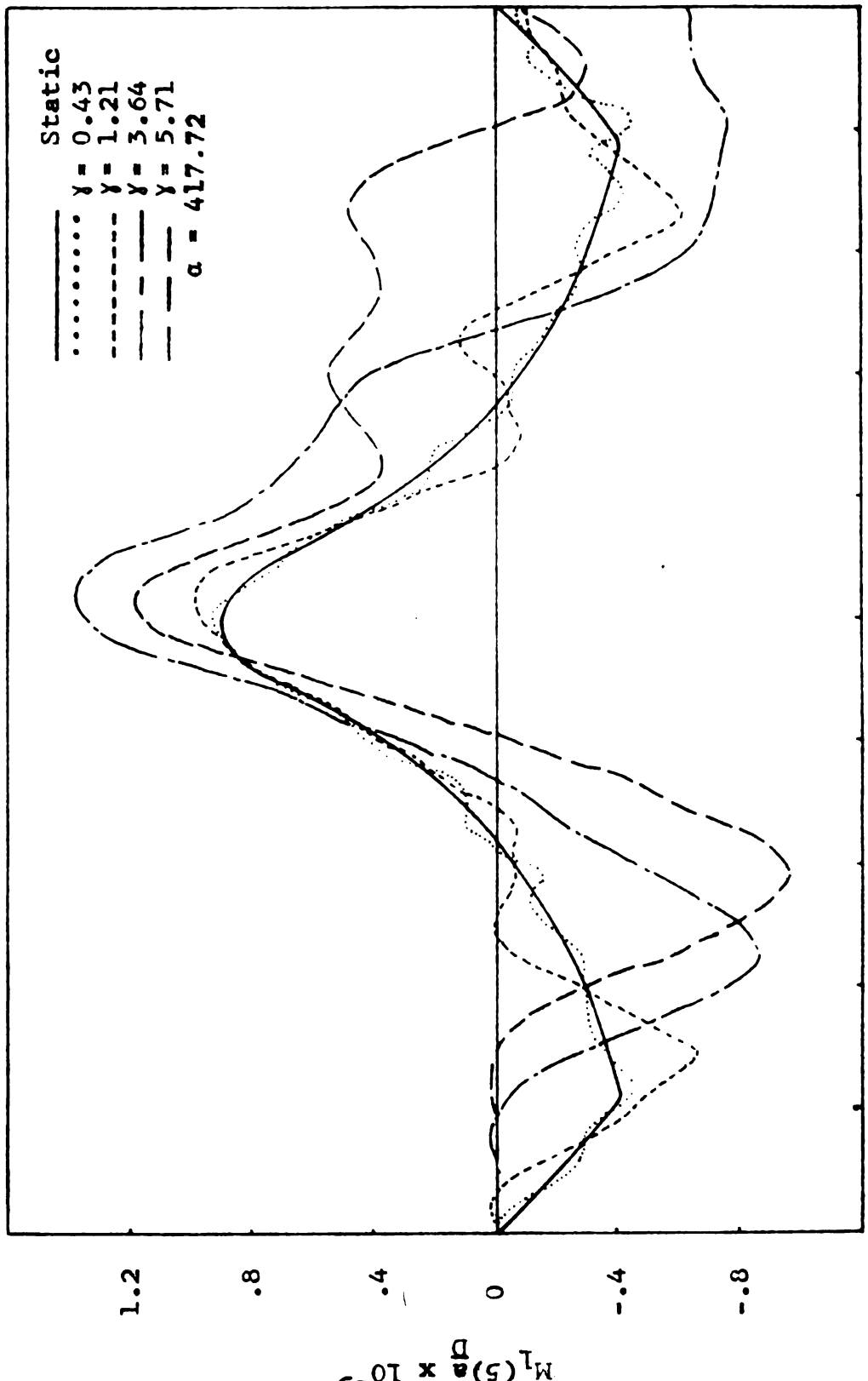

Fig. 3.7 MOMENT HISTORY CURVES FOR POINT 5 FOR VARIOUS VELOCITIES

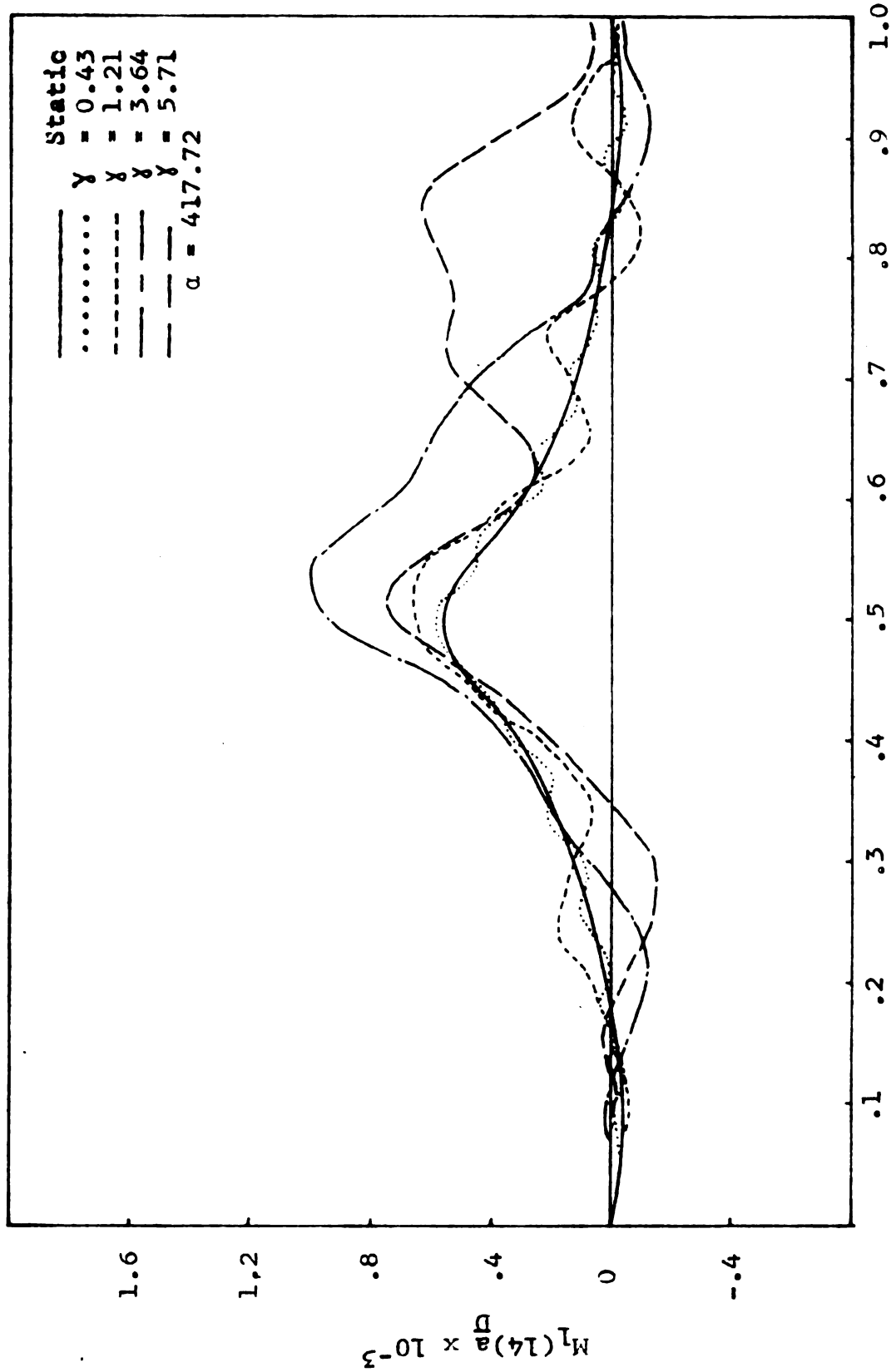

Fig. 3.8 MOMENT HISTORY CURVES FOR POINT 14 FOR VARIOUS VELOCITIES

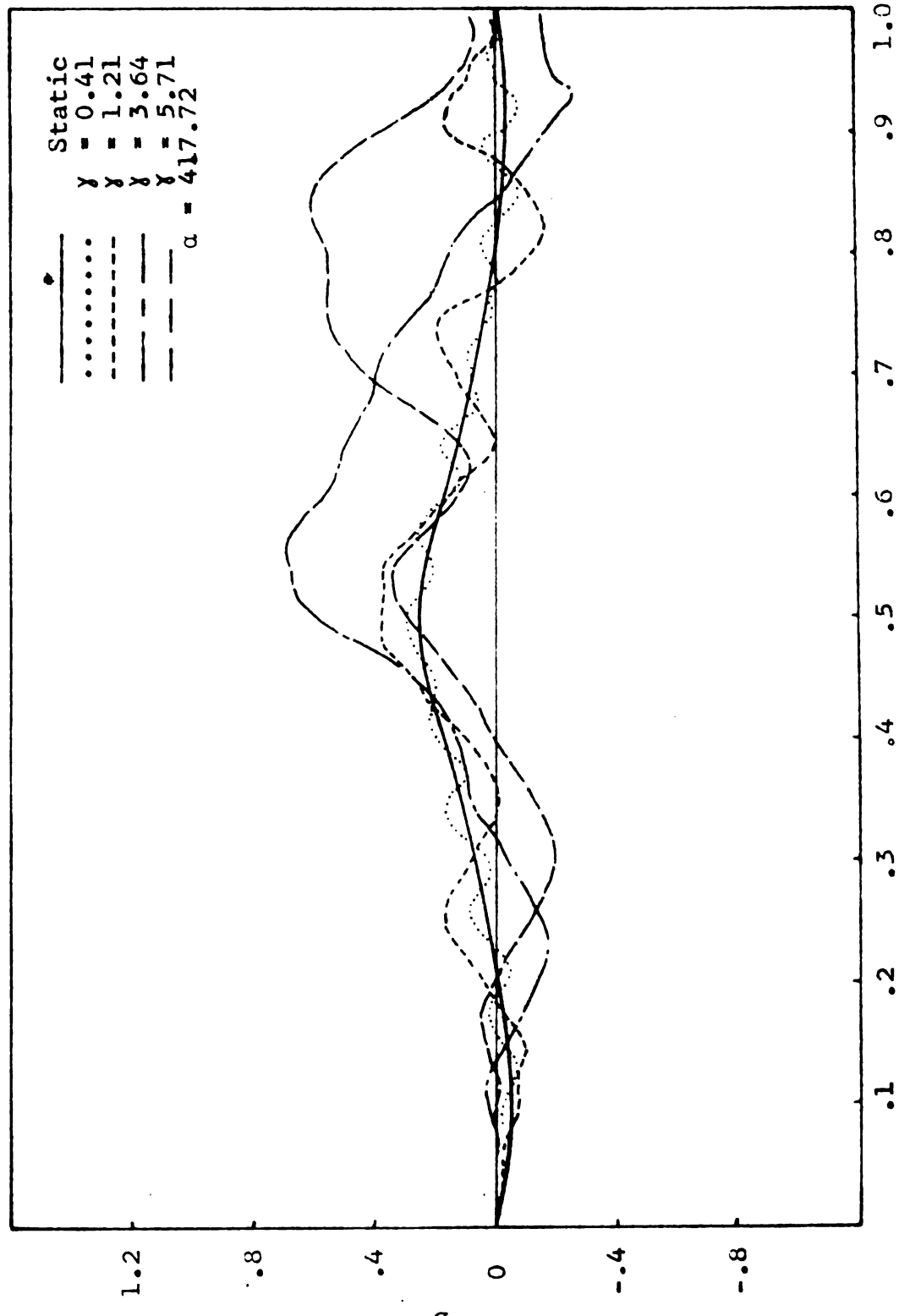

Fig. 3.9 MOMENT HISTORY CURVES FOR POINT 23 FOR VARIOUS VELOCITIES.

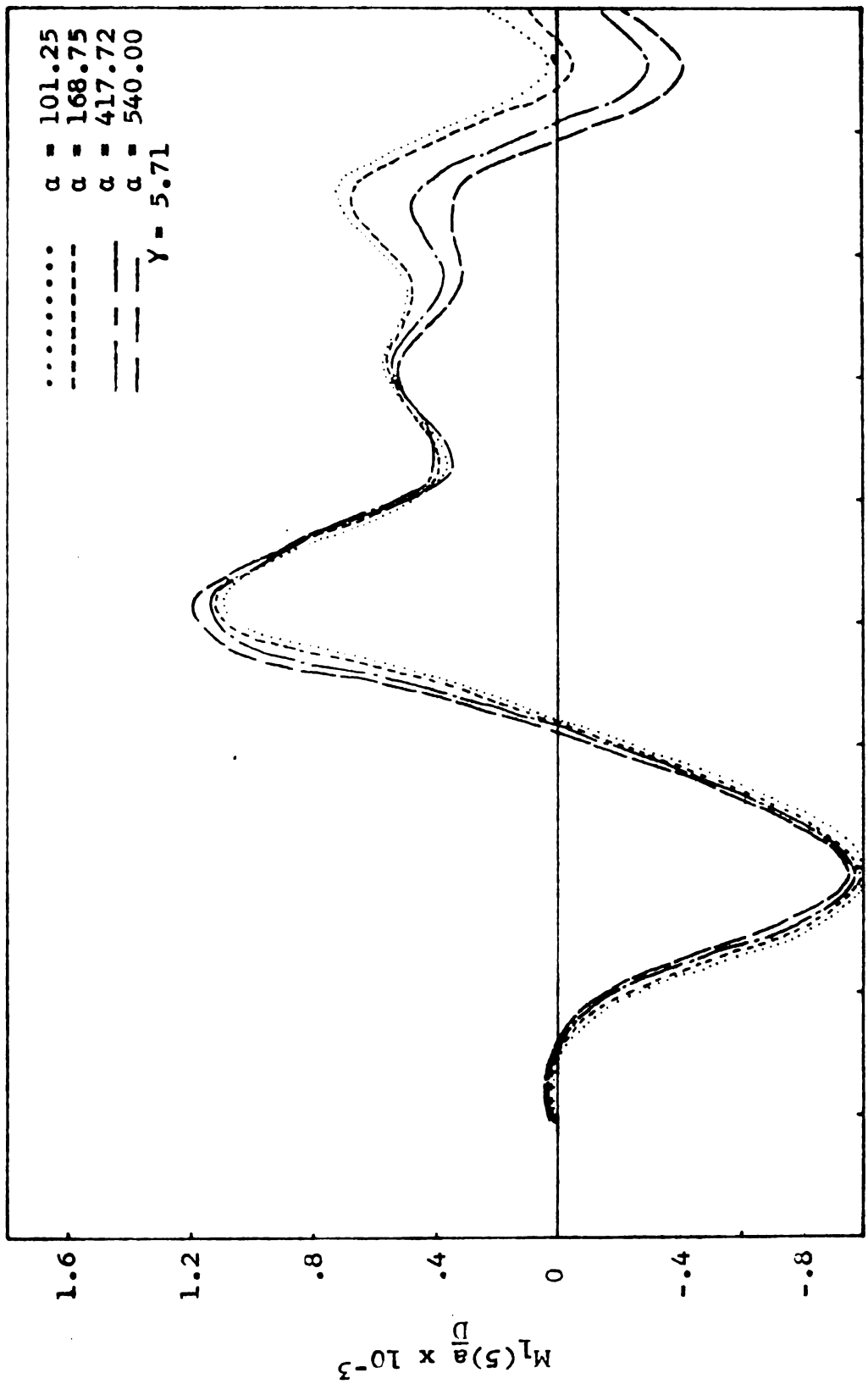

Fig. 3.10 MOMENT HISTORY CURVES FOR POINT 5 FOR VARIOUS FOUNDATION STIFFNESSES.

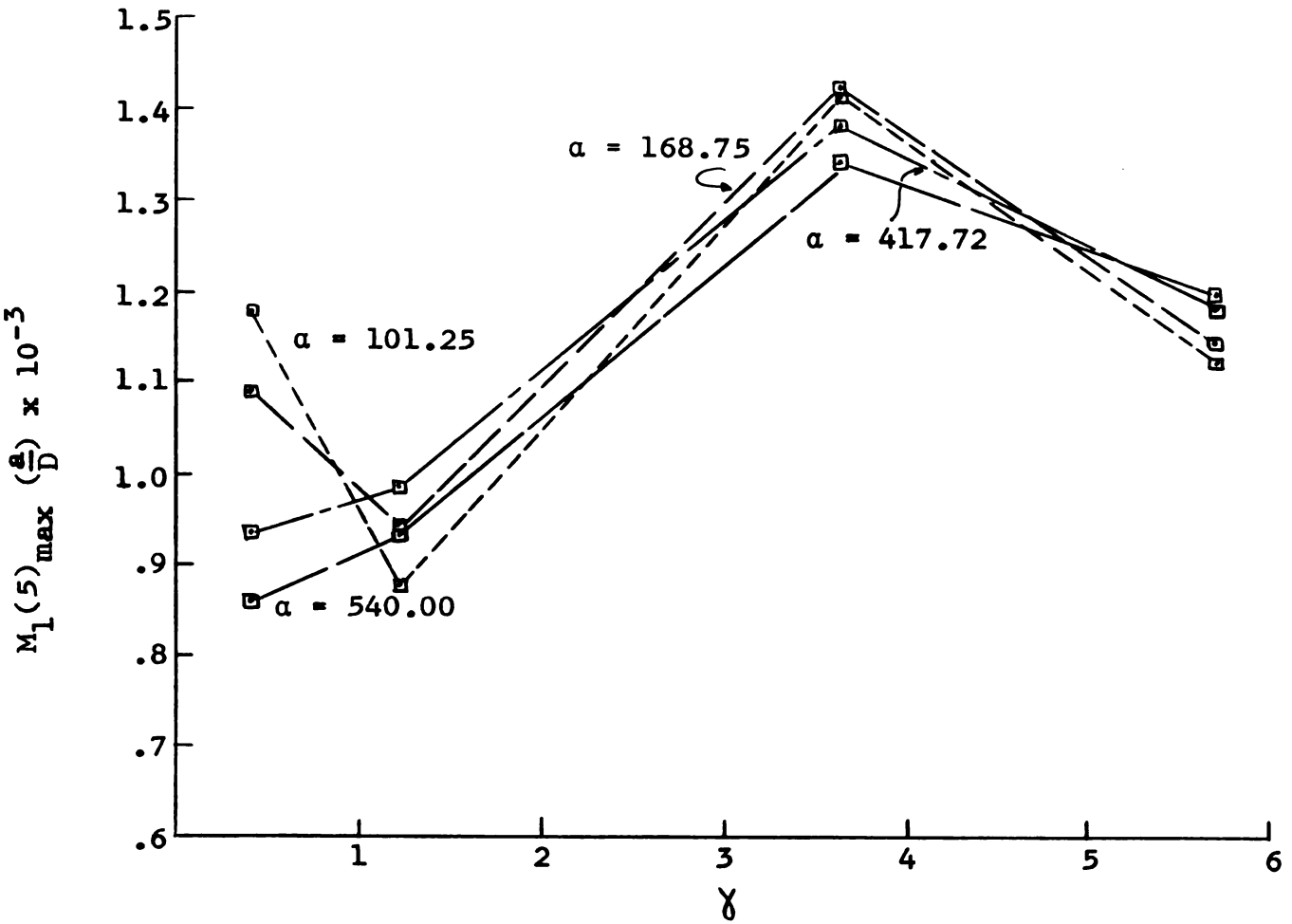

FIG 3.11 MAXIMUM MOMENT FOR POINT 5 VERSUS VELOCITY.

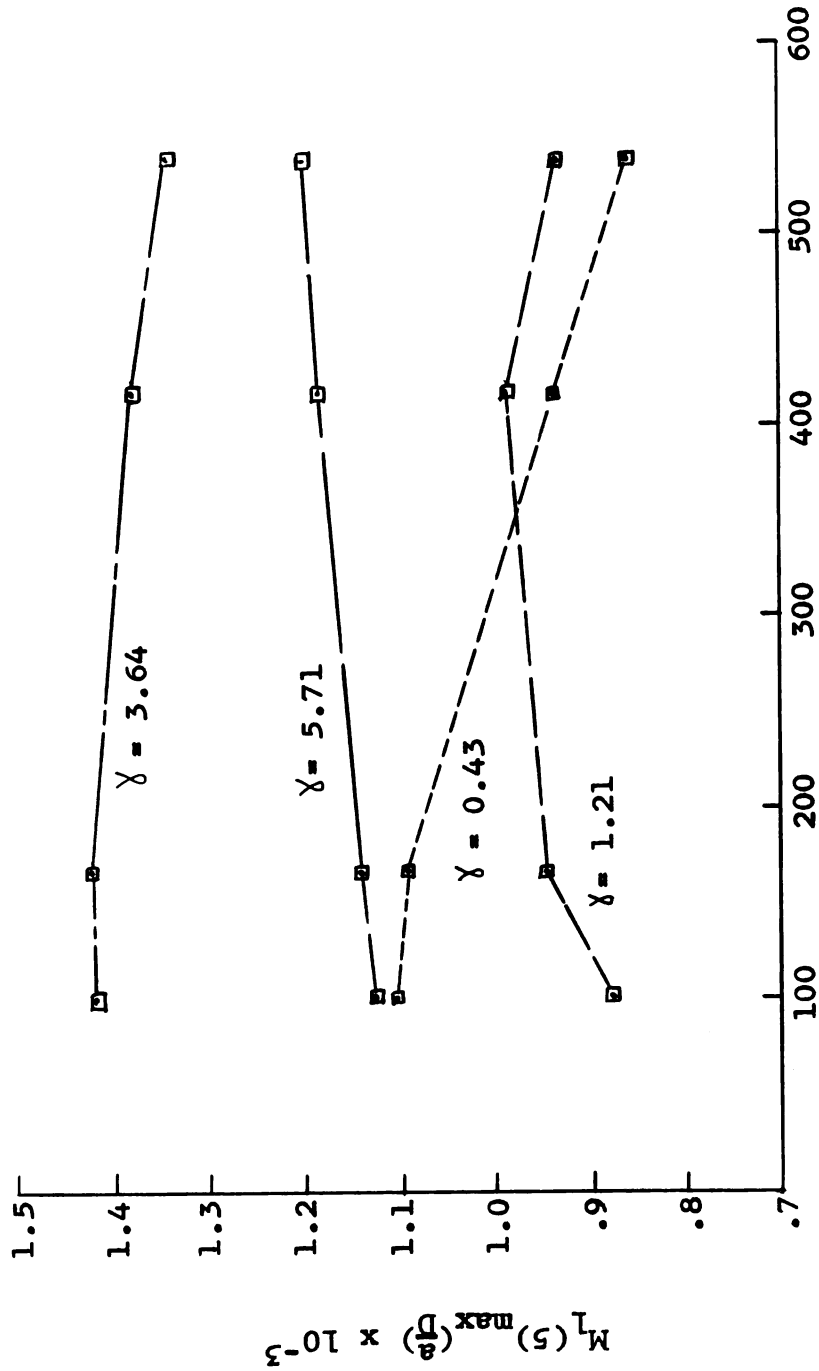

FIG. 3.12 MAXIMUM MOMENT FOR POINT 5 VERSUS FOUNDATION.

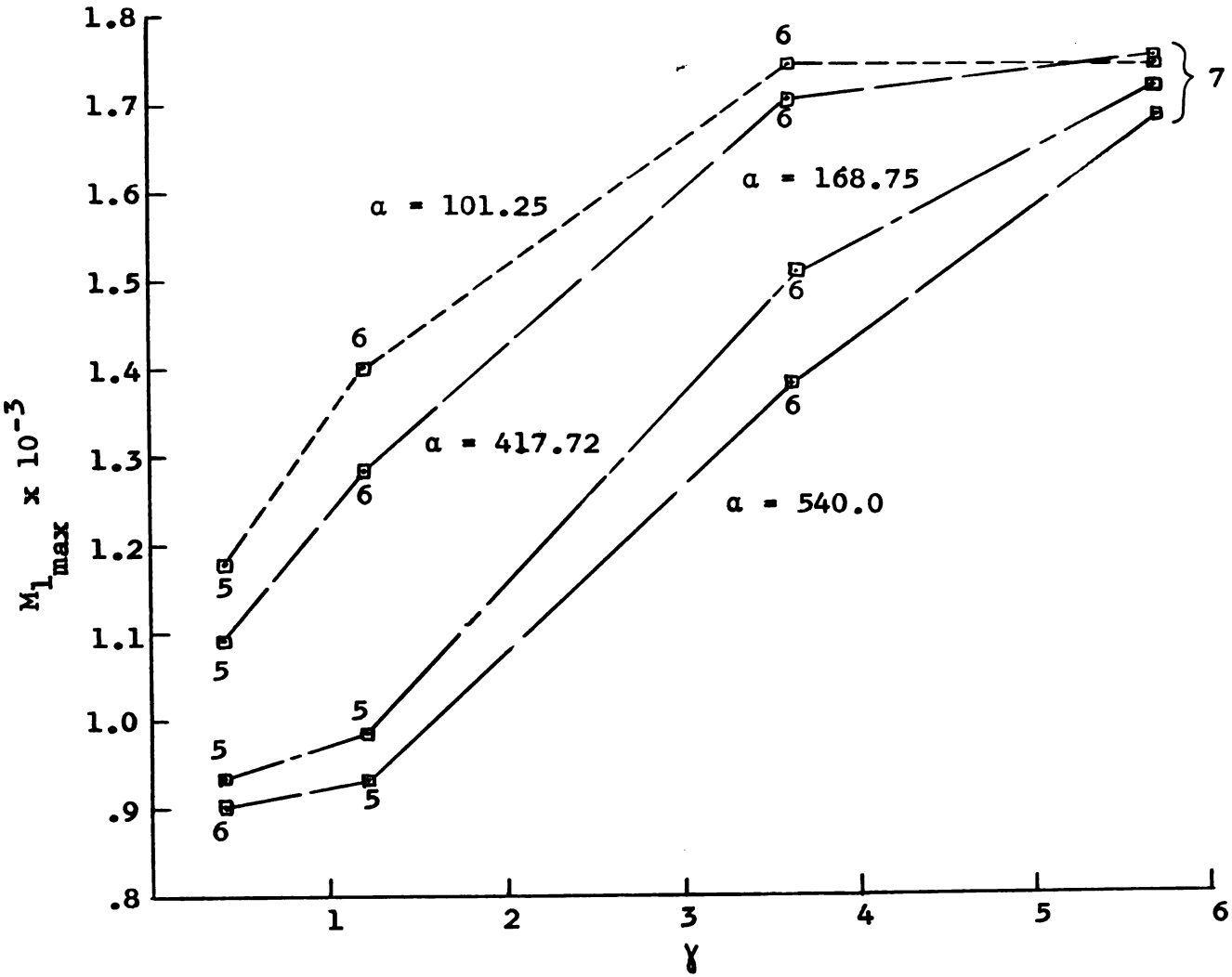

FIG. 3.13 MAXIMUM MOMENT IN PLATE VERSUS VELOCITY

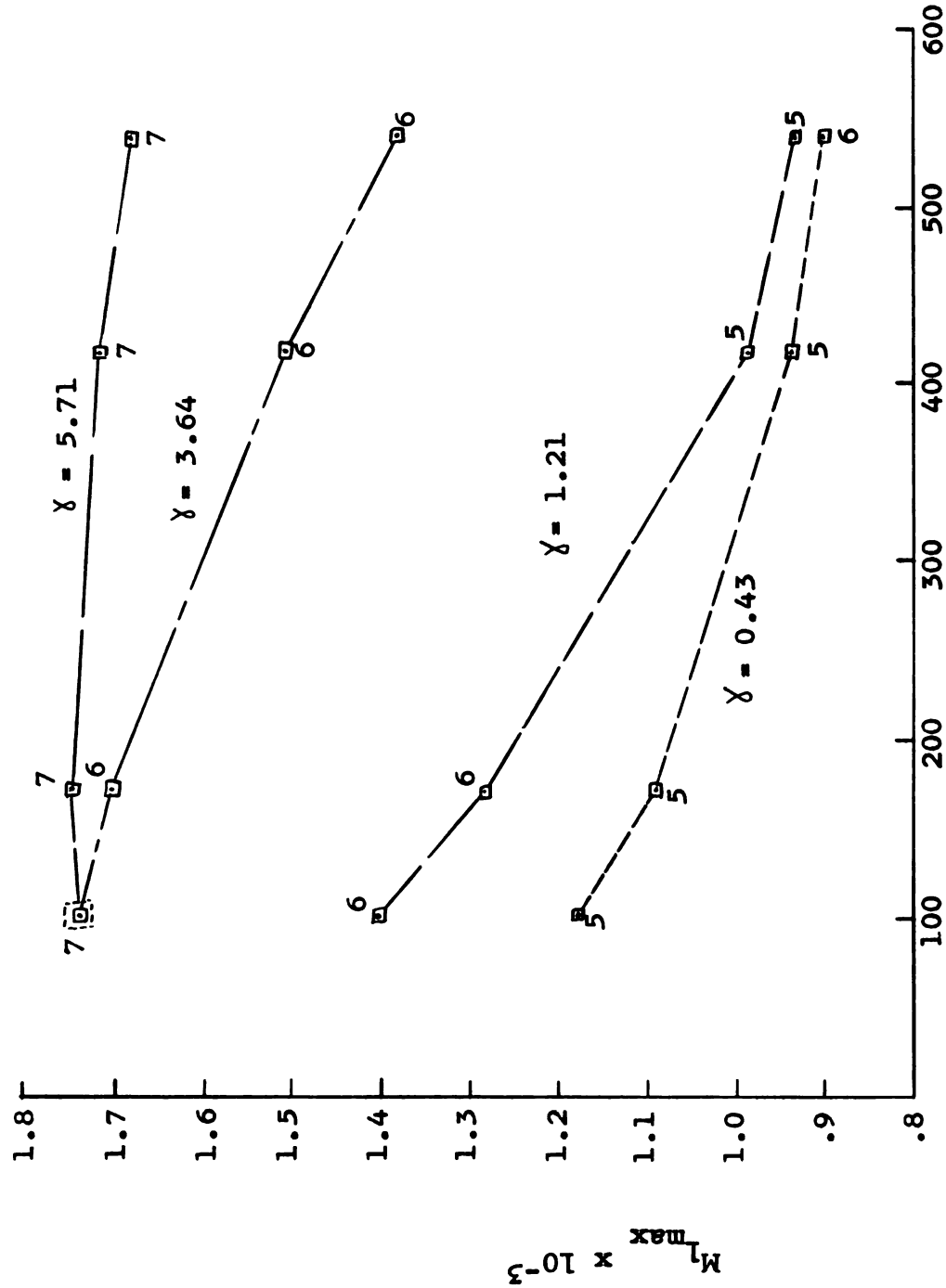

FIG. 3.14 MAXIMUM MOMENT IN PLATE VERSUS FOUNDATION

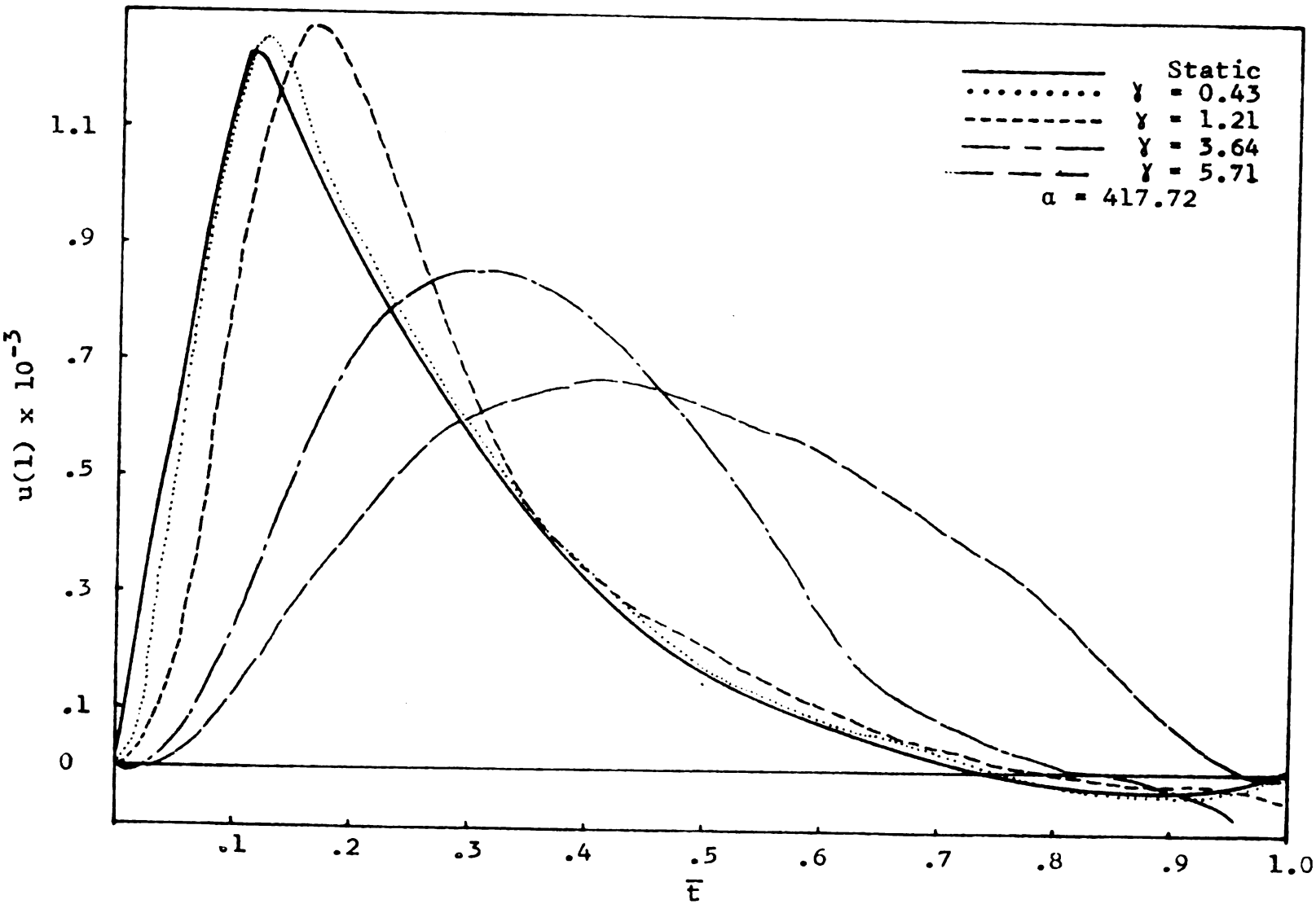

Fig. 3.15 DEFLECTION HISTORY CURVES FOR ENTRY CORNER FOR VARIOUS VELOCITIES WITH FOUNDATION DAMPING.

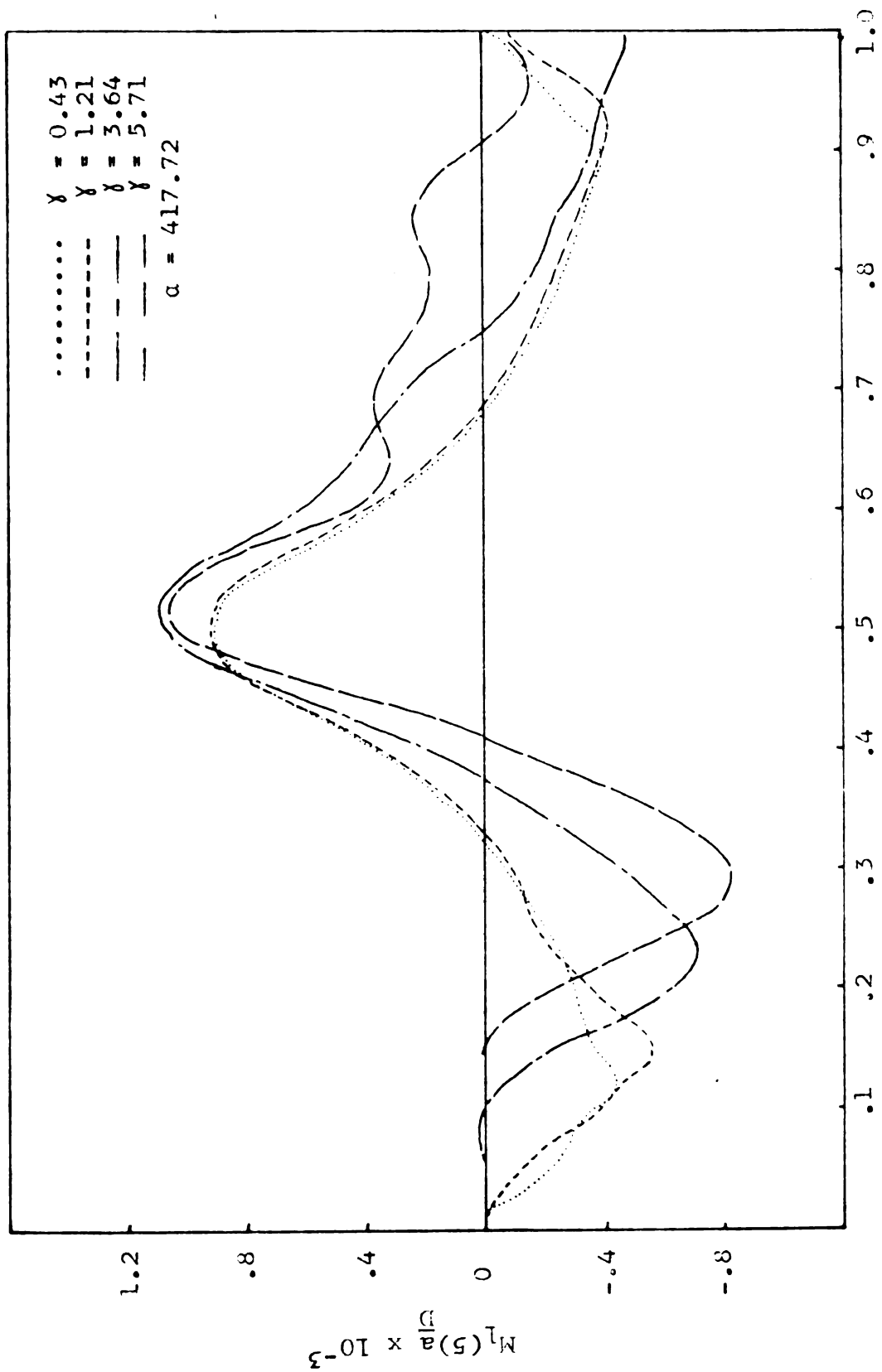

Fig. 3.16 MOMENT HISTORY CURVES FOR POINT 5 FOR VARIOUS VELOCITIES WITH FOUNDATION DAMPING.

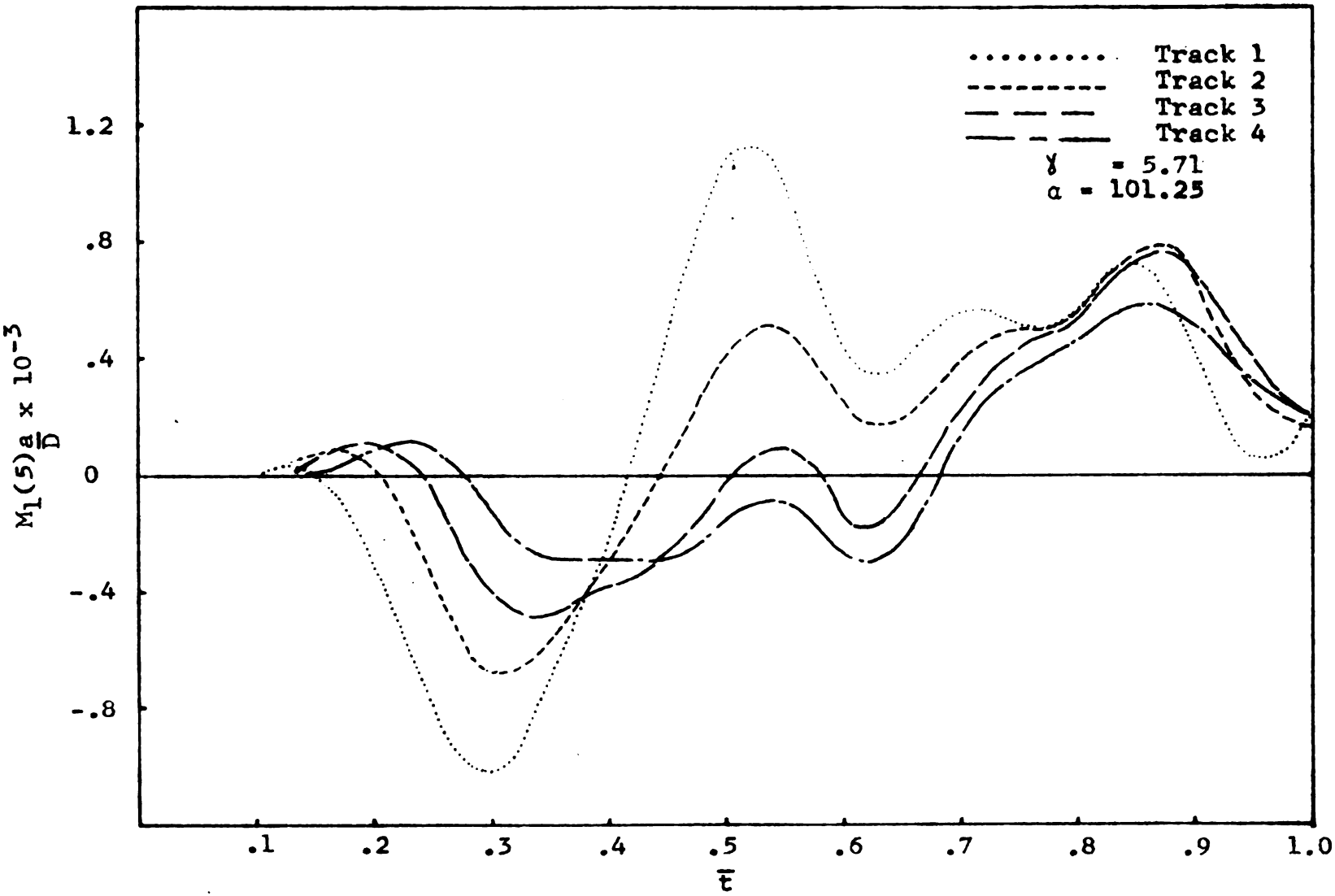

Fig. 3.17 MOMENT HISTORY CURVES FOR POINT 5 FOR VARIOUS LOAD TRACKS

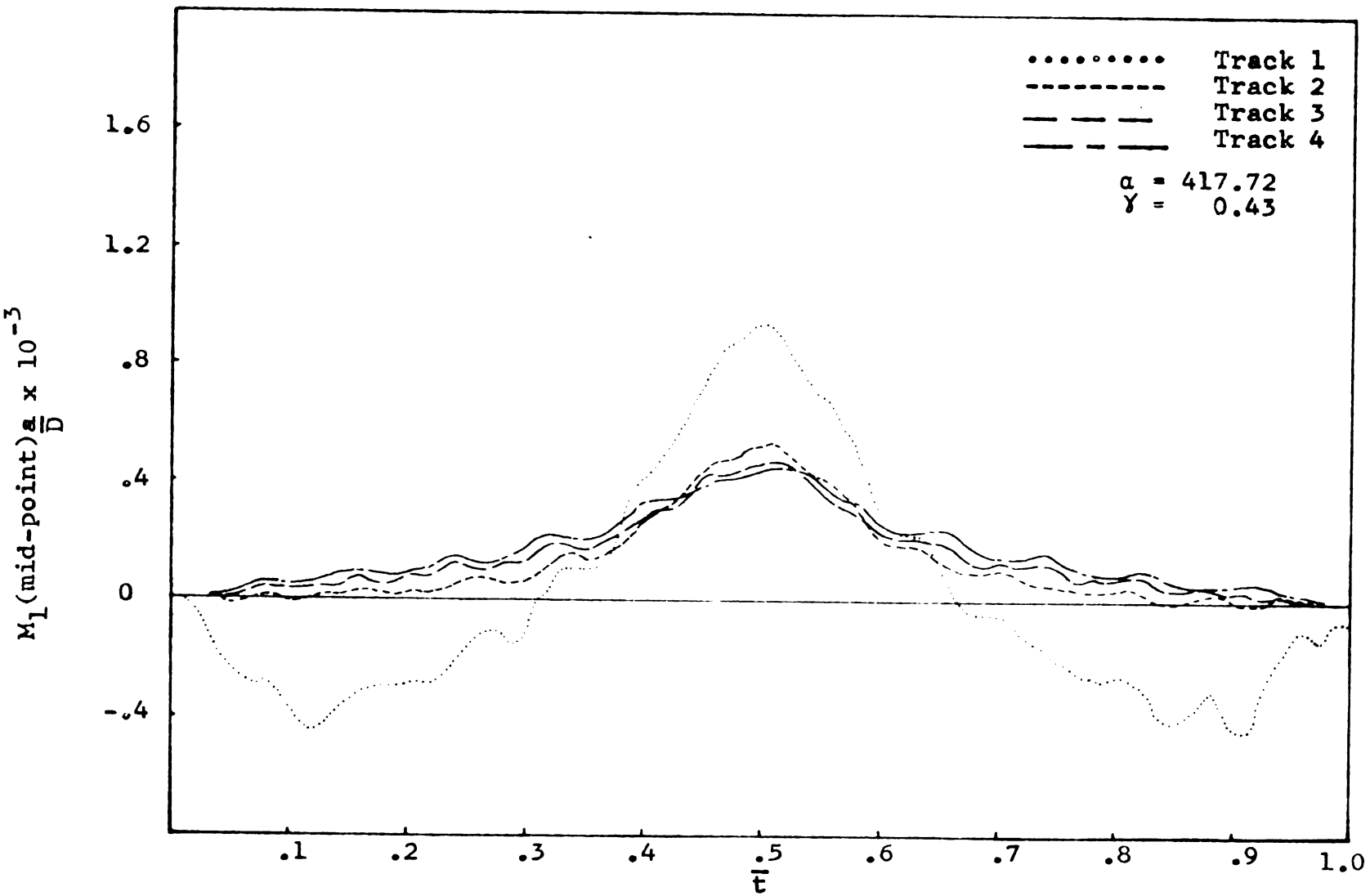

Fig. 3.18 MOMENT HISTORY CURVES FOR MID-POINT OF LOAD TRACK